University of
Stavanger

FACULTY OF SCIENCE AND TECHNOLOGY

MASTER'S THESIS

Study programme/specialisation: Engineering Structures and Materials - Master's DegreeProgramme	Spring/ Autumn semester, 2020 Open
Author: Alexander Thorkildsen	.... *Alexander Thorkildsen* .... Writer's Signature

Programme coordinator: Knut Erik Giljarhus Supervisor(s): Ove Mikkelsen Mostafa Ahmed Atteya

Title of master's thesis: Local joint flexibility of tubular offshore joints with eccentric brace to chord connections

Credits: 30

Keywords: Ansys Linear Nonlinear Parametric Optimization Local joint flexibility Tubular offshore joints Eccentric braces	Number of pages: 69 + supplemental material/other: 9 Stavanger, 30 June/2020

ABSTRACT

Local joint flexibility of tubular offshore joints has been researched to be able to account for correct deflection and redistribution of member forces and moments. This has shown to improve design life prediction for offshore structures. The literature reviewed in this thesis do not account for brace eccentricity in their equations. A study of the effect of brace eccentricity on tubular joints was therefore done. This involves a parametric study of around 200 linear static analysis of tubular T-joints. These were used to implement the eccentricity variable into Buitrago's out of plane bending equation. 28 nonlinear models were analysed in order to implement the eccentricity variable into MSL nonlinear ultimate capacity formula. After obtaining the results through finite element analysis. Regression and optimization were used to fit a function to the response generated by finite element analysis. Outcome from the linear static study resulted in a new equation with eccentricity that fitted the finite element analysis response with a R squared equal to 0.99. The nonlinear capacity equation with eccentricity achieved a R squared of 0.985. In both cases, there could be observed that the eccentricity factor did not have large influence on the local joint flexibility.

Table of Content

Table of Figures

List of Tables

List of Equation

List of Abbreviations

FEA – Finite element analysis

LJF – Local joint flexibility

DOE – Design of experiments

OSF – Optimal space filling

CCD – Central composites design

LHS – Latin hypercube design

APDL – Ansys parametric design language

1 Introduction

Great efforts have been done to establish a good basis for the calculation of local joint flexibility and strength capacity checks related to tubular joints. The work started in the 1970's with DNV and later came others like Efthymiou, Fessler and Buitrago to name a few. They generated flexibility equations based on lab test and numerical analysis. These formulations are applicable for linear elastic analysis, and they have shown to give a broad range of equations that can give reliable results for Y, K and X joints. Buitrago's equations are especially versatile. They also agree well with tested results like the Makino database, Buitrago's test included over 160 different joint configurations [1]. Later nonlinear pushover analysis was accepted as a method to determine loads that would generate deformation beyond the linear elastic area. Here MSL engineering did work alongside SINTEF to develop a code to be used in the USFOS computer program [2]. In this respect, loads from accidental, extreme wave and so on could be done with regards to global collapse or failure. But that demands the use of Pδ curves and plasticity models to be implemented [3].

All this research has contributed to extend fatigue life when reassessing structures. When designing structures, local joint flexibility will give a more accurate design and more knowledge about the behaviour globally and locally. And that is the main goal; to achieve high quality structures with high safety, to prevent the loss of life and material damages. The MSL report [4] with the example from Shell platform in the UK sector, gives an indication on the relevance the joint flexibility has in a structural analysis. This platform was chosen since a lot of magnetic particle inspections (MPI) results were available and a low fatigue life was documented when the reassessment was done. The fatigue life was under predicted using rigid joints. When implementing local joint flexibility (LJF), the fatigue life was more accurate and closer to what the inspection of the platform gave originally. Accounting for the LJF in the assessment of offshore jacket structures can, in this respect, contribute to improve the implementation of more efficient plans for damage inspection.
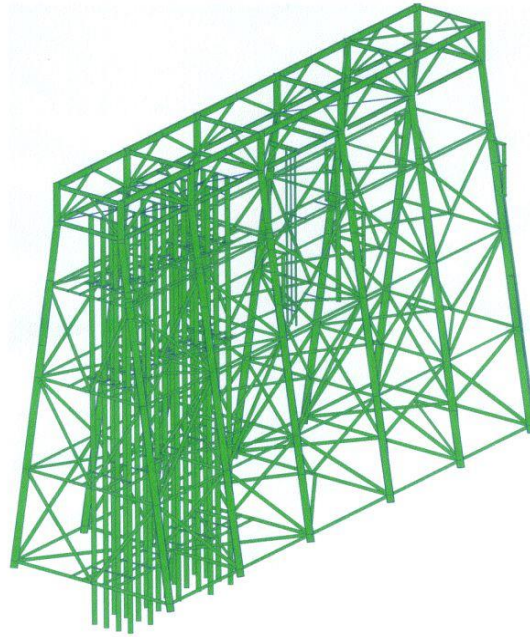
Figure 1 3D structure,"The effects of local joint flexibility on the reliability of fatigue life estimates and inspection planning"[4]

The eccentricity problem will be given a more detailed study in this thesis, compared to existing research. Then, corrections will be done to try to account for the effects of out of plane eccentricity. This will give the possibility to calculate capacity and deflection for this type of joints, which is not possible today. The main type of joints are covered, but problems can arise where this type of connection is necessary. Therefore, it will be easier to account for the effect through an equation. Today a full finite element analysis will be needed to check and verify problems with out of plane eccentricity. The reason why this has not been taken into the standards already, could be that the jacket structures mostly deal with in plane eccentricity and not out of plane. And the difference between in plane and out of plane eccentricity is shown in Figure 2.
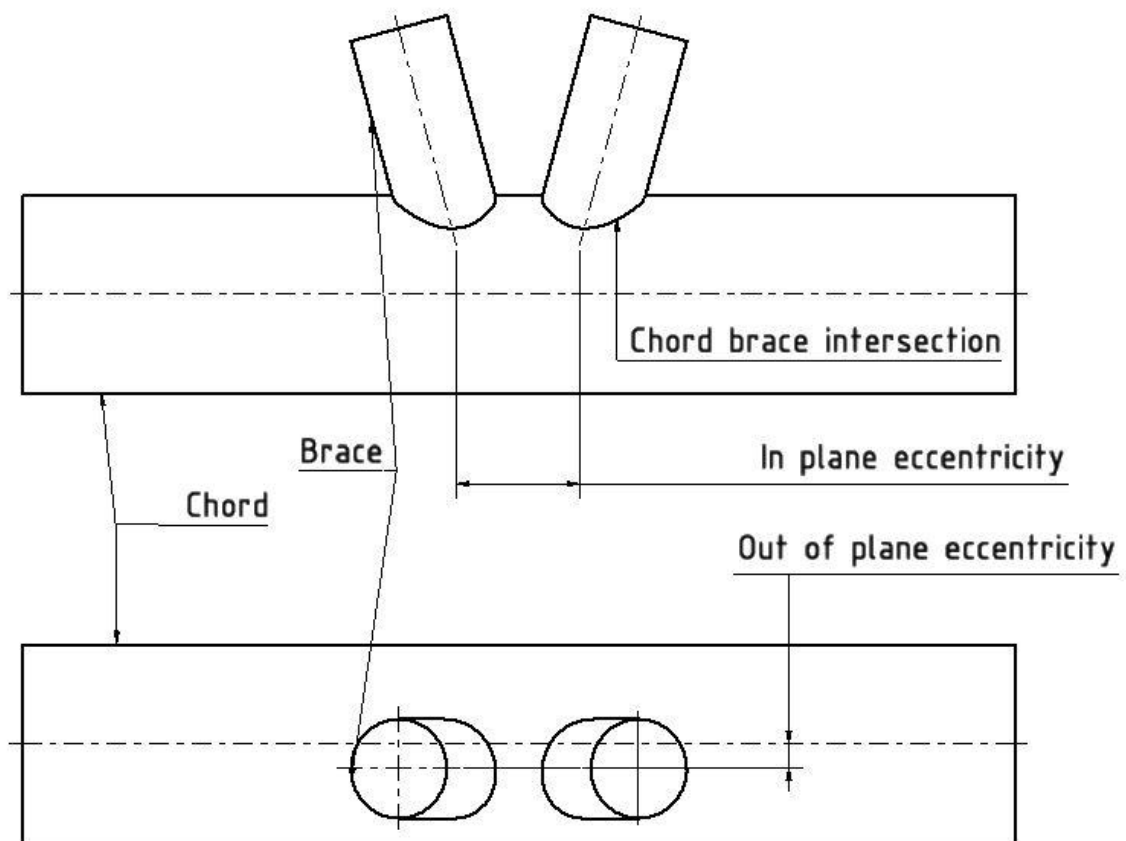
Figure 2 In plane- and out of eccentricity

The standards for design of offshore structures [5][6][7] accounts for the most common design needs, but do not consider any situation with out of plane eccentricity in tubular joints. More accurate analysis, data and research, to give guidance on how to account for the different types of conditions, are important as described above. This will require the same type of methods as used in the earlier research. A method must be chosen to create reliable results, and numerical finite element will be a natural choice. But the finite element analysis (FEA) will not be complete if you don't have good validation of the results and calibration of the input to the software. To do this, previous research will be compared to the FEA models.

3

2 Scope of work

- Matlab will be used to address all the empirical data and create all graphs. This will give a lot of data initially and validate what finite element model that will be appropriate to use.

- Beam, shell and solid models must be made to do validation. Here solving time, meshing and results will be important parameters.

- Study what weld stiffness could do to the results. Will that type of complexity be necessary to account for?

- Implement plasticity material and a solving algorithm that will handle the large deformations. Then the results of models here need to be verified against MSL nonlinear equation [3].

- Create a study of the eccentricity in the joint, when changing the constants for the tubular joints. Collect all the data results and compare with available empirical data.

- Expand the nonlinear capacity equation created by the MSL2000 report [3], by implementing eccentricity.

3   Literature

As an introduction to former research on tubular joint flexibility, a couple of the major contributors will be presented. A short resume on the research will be given. This will give insight to shortcomings of previous work and how it possibly can be used for validation. The equations presented will be for T/Y joints since these will be used to compare and calibrate the finite element models. For this a Matlab program will be made to check how these equations compares against each other and test. And with the curves generated in Matlab for the different LJF equations the finite element models can be calibrated.

3.1.1   DNV

In 1976 Det Norske Veritas published new equations which focused on local joint flexibility. At this stage the validity range are very narrow but considers in-plane bending and out of plane bending for t-joints. These equations are not very well validated against laboratory test, only finite element models. Still, they give an important start on the research to improve the flexibility of structures [1].

For T/Y joints:

$$LJF\ OPB = 5000(\gamma^{-1} - 0.01)^{(1.6\beta - 2.45)}/(215 - 135\beta)ED^3$$

$$LJF\ IPB = 18.6(\gamma^{-1} - 0.01)^{(1.5\beta - 2.35)}/ED^3$$

Equation 1 DNV LJF equations [8]

Validity range:

$10 \leq \gamma \leq 30$ $\qquad\qquad\qquad$ $0.33 \leq \beta \leq 0.80$ $\qquad\qquad\qquad$ $\theta = 90^{\circ}$

3.1.2   Efthymiou

Efthymiou started to work on improving DNV and Fessler work and tested a variety of joints. All his work is based on moment loaded K, Y and T joints, both in IPB and OPB. The equations he presented are purely based on finite element models with SATA software, and this makes his equations less reliable due to the missing experimental work. So, they will show to have mismatch with later experimental work. To be able to make equations one will need a large database to compare to and validate Fe software and the curve fitting [1].

For T/Y joints:

$$LJF\ OPB = 3.48\beta^{-2.12}\sin(\theta)^{(\beta + 1.3)}\gamma^{(2.2 - 0.7(0.55 - \beta)^2)}/ED^3$$

$$LJF\ IPB = 6.15\beta^{\left(-2.25-\frac{\gamma}{125}\right)}\gamma^{1.44}\sin{(\theta)}^{(\beta+0.4)}/ED^3$$

Equation 2 Efthymiou LJF equations [8]

10≤ γ ≤20   0.30≤ β ≤0.90   45 ≤ θ ≤ 90

3.1.3 Fessler

Fessler continued the work from DNV and improved the formulas and added a lot more range of the equation, he also added stiffness factor for joints in tension. The first set of equations did not have a published range. Later in 1986 Fessler made further improvement and added a new set of equations with a valid range of application [1].

For T/Y joints:

$$LJF\ Axial = 1.95\gamma^{2.15}(1-\beta)^{1.3}\sin{(\theta)}^{2.19}/ED$$

$$LJF\ OPB = 85.5\gamma^{2.2}\exp(-3.85\beta)\sin{(\theta)}^{2.16}/ED^3$$

$$LJF\ IPB = 134\gamma^{1.73}\exp(-4.52\beta)\sin{(\theta)}^{1.22}/ED^3$$

Equation 3 Fessler LJF equations [8]

Validity range:

10≤ γ ≤20   0.30≤ β ≤0.80   30 ≤ θ ≤ 90

All the equations were tested against earlier experimental work, also Fessler compared with Tebett's database from 1982. The equations showed to comply much better with the laboratory test. DNV and Efthymiou equations have flaws that will give lower stiffness in axial and a high stiffness for the OPB and IPB scenarios. So Fessler extensive work gives a more accurate estimate than these [1].

Fessler also presented a matrix to capture load scenarios from multiplanar and uniplanar joints. But at the time he did this work, the finite element software packages were not so sophisticated, and the computing resources were on a different level compared to today. This resulted in some differences in results on these equations for multiplanar and uniplanar joints, as an example some multiplanar joints may show differences up to 70%. The main reason for the criticism comes from that in his matrix formulation he ignored some terms, which perhaps had bigger influence than he thought [1].

3.1.4 Buitrago

Further research into LJF equations and joint flexibility were done through the years but in 1993 Buitrago did an extensive research [9], where he analysed 192 joints by FE software. Buitrago studied T/Y, K and X joints with axial and moment loads [1]. The IPB and OPB were included but the axial stiffness will be equal in tension and compression, this will not be entirely correct which can be seen when coming to MSL joint definition [3]. With respect to LJF the parameters β and γ have more impact than the θ and τ. Buitrago compared his results with the database used by Fessler. The database does not have enough tests to support all types of joint geometries. But Buitrago's FE models are assumed to give more accurate LJF estimates in that context. One shortcoming of his study is the gap in K joints, he had a hypothesis that with over 50mm gap the K joint exhibits Y joint behaviour. But he did not do a gap study to verify this theory [1].
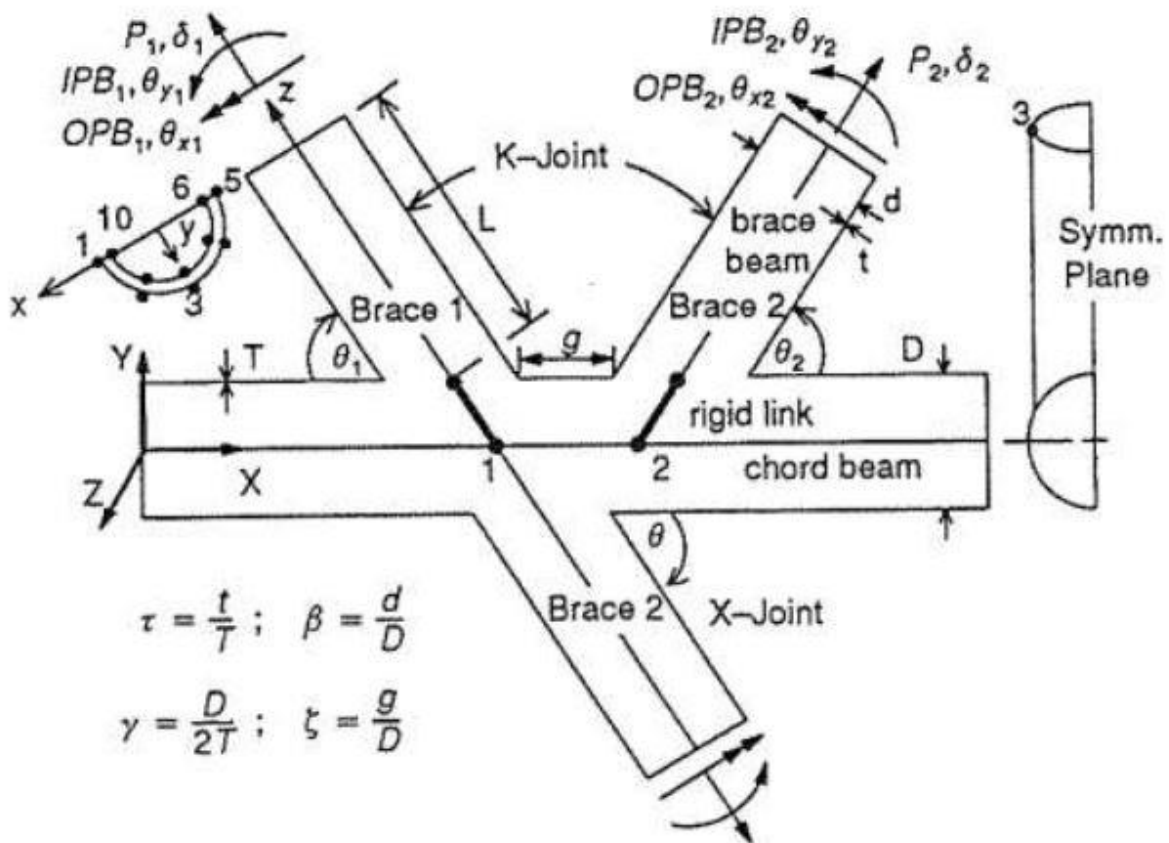
Figure 3 Joint," Local Joint Flexibility of Tubular Joints" [9]

Buitrago used shell elements to model and analyse his tubular joints, which gave the opportunity to develop the equations. They could then be efficiently used with a beam flex element in beam element programs. This means that the use of a rigid link and the short beam

flex element, gives the opportunity to change the second moment of inertia and area of the beam flex element according to the LJF equations. In beam element programs one can also insert a spring stiffness to simulate the behaviour and add beam offsets to give a more flexible joint. These different methods Buitrago tested did not differ with more than 10%. Buitrago concluded that this would lead to quite different distribution of forces and behaviour in larger structural analysis and would give more accurate analysis of structures [9]. His methods was later be implemented in frame analysis software, like SACS [4].

FOR T/Y joints:

$$LJF\ Axial = 5.69\tau^{-0.111}\exp(-2.251\beta)\,\gamma^{1.898}\sin{(\theta)}^{1.769}/ED$$

$$LJF\ OPB = 55\tau^{-0.22}\exp(-4.076\beta)\,\gamma^{2.417}\sin(\theta)^{1.883}/ED^3$$

$$LJF\ IPB = 1.39\tau^{-0.238}\beta^{-2.245}\gamma^{1.898}\sin(\theta)^{1.240}/ED^3$$

Equation 4 Buitrago LJF equation [9]

Validity range:

$10\leq \gamma \leq 30$ $\qquad\qquad\qquad\qquad 0.3\leq \beta \leq 1$ $\qquad\qquad\qquad\qquad 30 \leq \theta \leq 90$

$0.25\leq \tau \leq 1$

3.1.5   MSL joint

MSL engineering had two phases where research was done, the first phase gave a set of equations which later was improved. The research relies on finite element modelling, then verified against Makino, Korubane, Boone and the BOMEL frame tests. The first phase involved a large work with collecting test data and numerical data, then to work through this to get the reliable results. From this the work could start to create the mathematical equations and algorithms to represent the force/deflection curves. The mathematical equations for the axial(P) and moment(M) curves were created and tested to fit for different types of geometry and material [1].

Phase two did first improve on the influence of the different geometry factors, and the chord/brace interaction, classification of joints, coupling between moment and axial loading, unloading behaviour and limits with regards to deflection. After this benchmarking of the

equations was carried out, and the formulations showed to give more flexibility and in good agreement with the large-scale frame tests [1].

The main goal to be achieved with the MSL joint formulation was to get a strength capacity check, more correct flexibility of the joint, joint moment and forces, global response and to help with the fatigue assessment. There is no guide in the MSL on fatigue, but the flexibility will result in changes for the stress concentrations occurring in the joint, from this a more accurate estimation can be given for the lifetime on frame structures. The MSL formulation also need to be implemented into a structure program, and here MSL and SINTEF used the USFOS software package to implement the MSL joint module [3]. The strength check and the flexibility improvement added for joints to this program will improve the global response and load distribution better than with rigid joints. The strength check will also give confidence that the structure can handle the loads or if it needs to be revised. But there are some factors that needs to be changed during the loading scenarios with the MSL module due to that plasticity is allowed. The first factor is the joint classification, the classification can change due to the deflection and load redistribution. The second is the Qf factor, which represents the chord load action, this will also need to be updated along with the simulation [3]. How well this is handled in a software will be up to the programmer, but an efficient way will be important.

The uncoupled Pδ and Mθ equations are presented below, this were also used to get the interaction between axial and bending loading scenarios, along with the hardening rule to change the yield surface. The interaction strength check will differ for what type of code the program will check against, also small changes in parameters will change for the uncoupled curves depending on the code [3].

MSL Linear/nonlinear uncoupled:

$$P = \phi P_u (1 - A\left[1 - \left(1 + \frac{1}{\sqrt{A}}\right)\exp\left(-\frac{B\delta}{(\phi Q_f F_y D)}\right)\right]^2)$$

$$M = \phi M_u (1 - A\left[1 - \left(1 + \frac{1}{\sqrt{A}}\right)\exp\left(-\frac{B\theta}{(\phi Q_f F_y)}\right)\right]^2)$$

$$K_{ini}P = 2P_u(1 + \sqrt{A})\frac{B}{DF_y Q_f}$$

$$K_{ini}M = 2M_u(1 + \sqrt{A})\frac{B}{F_y Q_f}$$

MSL coupled Pδ and Mθ interaction equations:

$$\Gamma = (\frac{N}{R_N N_0})^{\alpha 1} - \left(\left(\frac{M_{ipb}}{R_{ipb}M_{0,ipb}}\right)^{\alpha 3} + \left(\frac{M_{opb}}{R_{opb}M_{0,opb}}\right)^{\alpha 4}\right) - 1$$

When the analysis has both bending and axial loading, the force axes will move and the interaction surfaces will change due to the force components softening or hardening.

3.2 Joint classification

The classification does not reflect on geometry but by the balancing of forces and what type of stress behaviour the joint experience. Looking at the geometry will give an indication, but the force balance and stress behaviour needs to be checked to account for the correct joint. In the standards a weighted average can be taken if a joint shows behaviour that needs multiple classes.

All the classification is done from plane to plane, braces that is ± 15 deg from the plane considered, can be assumed to be in the same plane. Also, a force that is within 10 percent of load balance is to be classified as entirely one. But some joints can become complex and difficult to classify, but numerical finite element can now be validated against test and then used to calculate the effects in the joint with relative high safety. The only problem is the tension failure in the joint, because here a failure criterion does not yet exist. For these cases tests need to be addressed to be able to determine the capacity of the joint.

The types below are the main classifications that the standards will address, the important thing is to follow the forces through the joint and classify from that and not geometry. Problems to clarify what classification the joint has can come when the complexity increase and when multiple load cases need to be driven for an analysis, the classification can change due to the loading. This must be implemented in a type of code check for the frame analysis programs.

T/Y: Classified by shear force in the chord member and are not balanced by other forces in the chord.

K: Classified by braces that balances each other forces in the connection, from the same side of the chord.

X: Classified by braces that balances each other's forces from opposite of the chord member.

An example is if the joint is a DT or X joint, her beta(β) ratio will affect the decision. Because the joint will be a X joint if the forces a transferred to the other brace and not locally taken up by the chord. From the ISO 19902 [7] the X joint has a $Q_u = 23\beta$ for β ratios below 0,9, and the T/Y $Q_u = 30\beta$. What classification should be used in cases where the values of β are close to each other. Then one need to check by FEA or other methods to get confidence in what the different choices does to the capacity. But as seen later in the thesis a comparison between DT joint from numerical and empirical calculations will be made, with the β=0,4. Then the joint will be expected to transfer the forces through the chord wall.
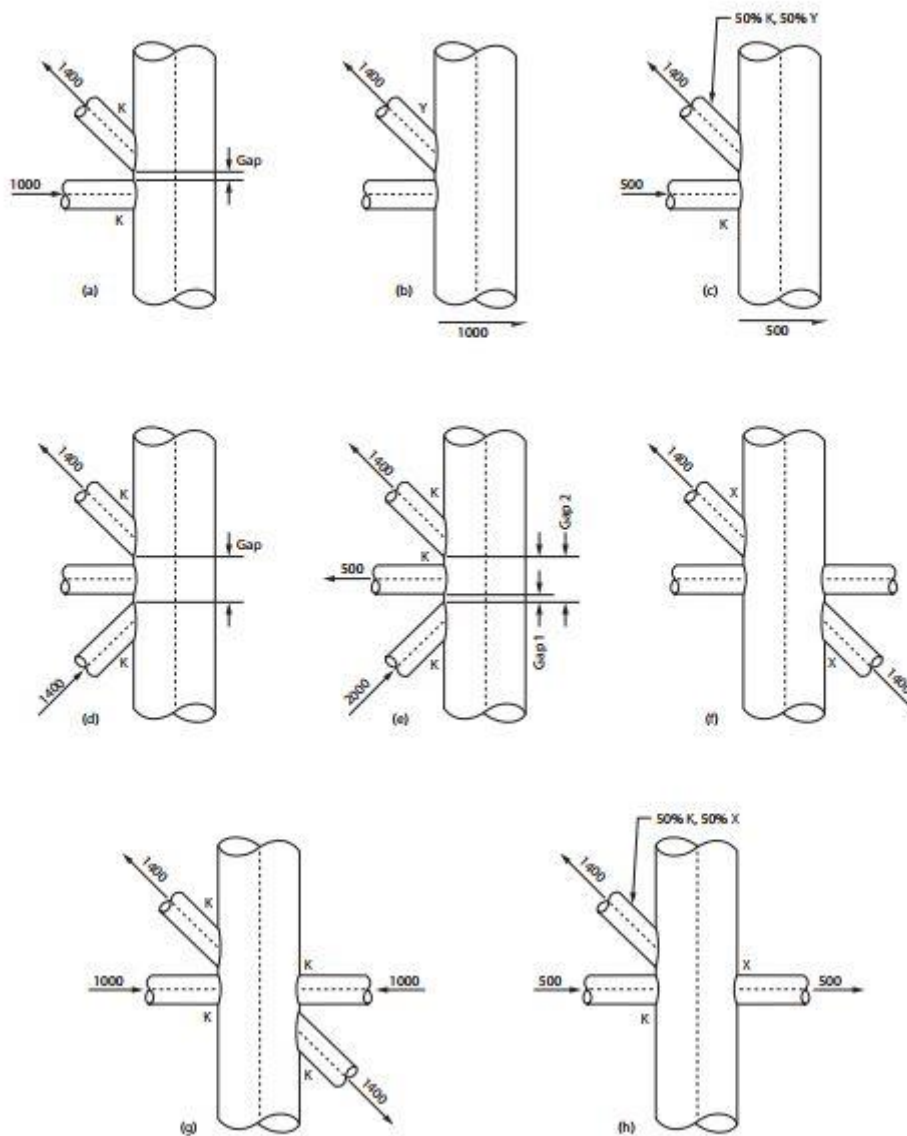
Figure 4 Different joint classifications [5]

Figure 4 shows a couple of examples of classification, and one can see that if a large structure should be calculated, a code to do this will be beneficial. The knowledge to check the code will still always be necessary, and to know when more detailed analysis will be required to provide validation of a complex joint.

3.3 Standards

There are three main standards used in the industry for capacity and code checking of tubular joints. These are API RP 2A LRFD [6], ISO 19902 [7] and Norsok N-004 [5], they will have small differences but a knowledge of all will give the best overview of the limitations for the calculations of tubular joints. The formula for basic resistance is similar in all the standards

12

and the validity range, some deviations comes when multiplanar joints are of concern. The standards take care of calculation procedures for simple joints and gives advice on good engineering practice when it comes to choices related to joints.

Basic resistance, strength criteria and validity range:

$$N_{RD} = \frac{f_y T^2}{(\gamma_M) sin\theta} Q_u Q_f$$

$$M_{RD} = \frac{f_y T^2 d}{(\gamma_M) sin\theta} Q_u Q_f$$

$$\frac{N_{Sd}}{N_{Rd}} + (\frac{M_{y,Sd}}{M_{y,Rd}})^2 + \frac{M_{z,Sd}}{M_{z,Rd}} \leq 1$$

$$0{,}2 \leq \beta \leq 1$$

$$10 \leq \gamma \leq 50$$

$$30° \leq \theta \leq 90°$$

$$F_y \leq 500 \, MPa$$

$$\frac{g}{D} > -0{,}6 \, (K \, joints) \rightarrow N - 004 \, and \, API \, RP \, 2A$$

$$gT > -1{,}2\gamma \, (K \, joints) \rightarrow ISO \, 19902$$

Equation 7 Basic tubular joint capacity [5][6][7]

Also, the main parameters that will be needed for setting up the equations and check the joint validity range to, are displayed in the standards.
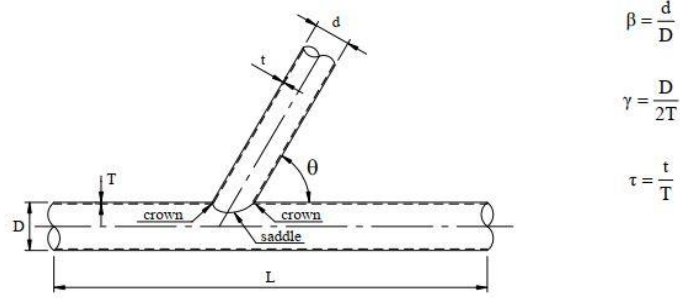
Figure 6-3 Definition of geometrical parameters for T- or Y-joints

$$\beta = \frac{d}{D}$$

$$\gamma = \frac{D}{2T}$$

$$\tau = \frac{t}{T}$$
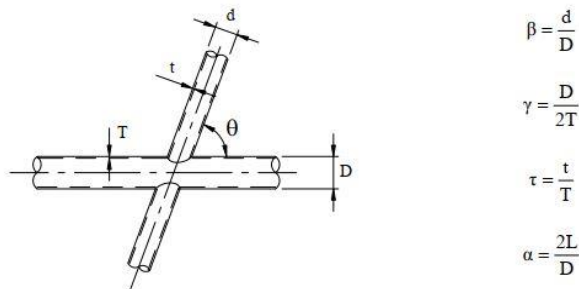
Figure 6-4 Definition of geometrical parameters for X-joints

$$\beta = \frac{d}{D}$$

$$\gamma = \frac{D}{2T}$$

$$\tau = \frac{t}{T}$$

$$\alpha = \frac{2L}{D}$$

Figure 5 "Geometrical parameters for T-/Y- and X-joints" [5]
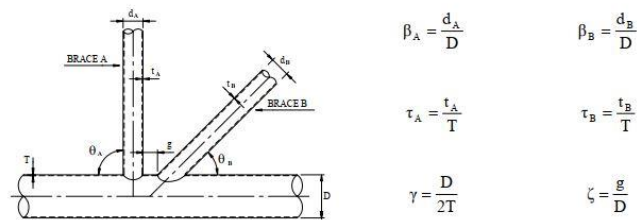
Figure 6-5 Definition of geometrical parameters for K-joints

$$\beta_A = \frac{d_A}{D} \qquad \beta_B = \frac{d_B}{D}$$

$$\tau_A = \frac{t_A}{T} \qquad \tau_B = \frac{t_B}{T}$$

$$\gamma = \frac{D}{2T} \qquad \zeta = \frac{g}{D}$$
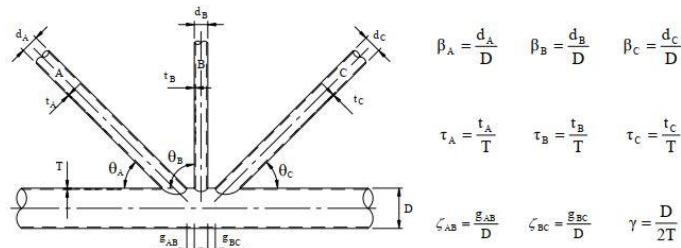
Figure 6-6 Definition of geometrical parameters for KT-joints

$$\beta_A = \frac{d_A}{D} \qquad \beta_B = \frac{d_B}{D} \qquad \beta_C = \frac{d_C}{D}$$

$$\tau_A = \frac{t_A}{T} \qquad \tau_B = \frac{t_B}{T} \qquad \tau_C = \frac{t_C}{T}$$

$$\zeta_{AB} = \frac{g_{AB}}{D} \qquad \zeta_{BC} = \frac{g_{BC}}{D} \qquad \gamma = \frac{D}{2T}$$

Figure 6 "Geometrical parameters for K- and KT-joints" [5]

The Qu and Qf factors will also be given recommendations in the standards, these will change due to the classification. But for multiplanar joints API [6] gives more guidance into these factors than ISO 19902 [7] and N-004 [5]. The information available in the standards often

14

comes down to how much data on the different geometries and test done. And more information and test can refine and improve the methods and the empirical formulas. This seems to be the major difference between the standards, API [6] have done more testing and have built a larger database. One also gets recommendations regarding thin walled and tension loading with high strength steel, which can go beyond the first crack principal used. In the USFOS theory deformation limits was introduced to check against, based on the first crack initiation [2]. API [6] also gives more recommendations regarding the multiplanar joints, since the classifications schemes can become difficult to use and not give reliable results. API gives some references to CIDECT guide and AWS. AWS has an approach that one looks at the ovality of the joint and the angle related to where braces are connected. The API standard goes more into depth to clarify and to give more information related to what limitations and paths to be taken in different scenarios. ISO 19902 and N-004 do not give as much information as API but gives guidelines and when followed, a safe design will be achieved. And here the safety calibration comes into play, which is described in API, but some of the equations in ISO 19902 and N-004 implements some safety factors and a part of the factors are also implemented into the Qu and Qf factors in all the standards.

Another common thing through every standard is that the chord must be the last member to fail, because of the importance that these members have in the structure. Therefore, multiple options will be presented to strengthen them. The most common ones are ring stiffeners or thickened cans. These methods will give the chord a lower utilization but can affect fatigue life of the structure with the way forces will be transferred through the joint. But ring stiffeners today do not have a good guide in the standards and more effort needs to be put into research and implementation.

3.4   Joint flexibility

Methods used for calculating load deformation curves and local joint stiffness or capacity is today hand-calculations from standards or LJF from earlier research as Buitrago [9], the other method is finite element analysis. Hand-calculation is a good way to get confident with the values produced for instance by finite element method. The formulas for this are presented earlier in the thesis, now the focus is on how to do this by finite element analysis, and how these stiffness factors can be calculated using a software like Ansys. The theory of the finite element method will also be of importance here, since the choice of elements, integration and solving procedures will affect solution accuracy and time.

The local joint flexibility factors are intended to be used in connection with finite element programs based on beam elements. These stiffness factors can be found in a specific way and presented here is Buitrago's method [9] which is the common way. Because it is the local joint flexibility that will be interesting to bring into a frame program. First a presentation of Buitrago's [9] way will be presented. This is important to understand through all work with joints. Because if it is not understood, all measured values and comparisons will not make sense. The deformation that will be important is the local net deformation, this will be the total deformation and then subtract the beam deformations.

$$f_{axl} = LJF_{axl}ED = (\delta_z^{brace} - \delta_{axl}^{brace} - \delta_{axl}^{chord})\frac{ED}{P}$$

$$f_{ipb} = LJF_{ipb}ED^3 = (\theta_y^{brace} - \theta_{ipb}^{brace} - \theta_{ipb}^{chord})\frac{ED^3}{M_I}$$

$$f_{opb} = LJF_{opb}ED^3 = (\theta_x^{brace} - \theta_{opb}^{brace} - \theta_{opb}^{chord})\frac{ED^3}{M_O}$$

$$P, M_I, M_O = Loads\ Axial, In\ plane\ bending, Out\ of\ plane\ bending$$

$$\delta_z^{brace}, \theta_y^{brace}, \theta_x^{brace} = brace\ end\ deformations$$

$$\delta_{axl}^{brace}, \theta_{ipb}^{brace}, \theta_{opb}^{brace} = brace\ beam\ end\ deformations$$

$$\delta_{axl}^{chord}, \theta_{ipb}^{chord}, \theta_{opb}^{chord} = chord\ beam\ deformations\ at\ brace\ intersection$$

Equation 8 Buitrago nondimensional factor [9]

To do this measurement first a beam model must be built, setting up the chord and the brace, also an offset need to be built to represent where the intersection point between chord and brace are. Here a rigid link will be needed to take care of this. Then the deformations can be taken out from the nodes at the actual points of interest. Then if a solid finite element method is used to take the other measurements, an approach of calculating the algebraic difference of node translation in the actual plane, this needs to be done each side of the brace and the divided by the brace diameter [9]. Both at the end and the intersection this method must be used to extract results. Especially for solids since those elements do not have rotation degrees of freedom. The same procedure can be used for shells, but also in the software today you can extract the rotation results directly, since shells contains rotational degrees of freedom. For the

axial displacement a nodal average of ten nodes should be used, this will be chosen around the brace end circle [9]. All these representations are shown in Figure 3.

4 Theory

4.1 Finite element concepts

The finite element theory is a very important part of this thesis, since Ansys will be used extensively. A presentation of mathematical fundamentals that will be presented here are from [10]. Ansys's exact code is not available in the theory manual but the principals will not be different. They have of course their own experience from test and interpretation, and this will naturally affect what they have implemented in for example elements and solution algorithms to improve performance. But a fundamental understanding of the field will give an excellent way to interpret what options Ansys gives and what is needed to perform the analysis. This will help when reading the manual for the program which must be used often to get a clear understanding of limitations and possibilities with the setup. Today much is being automated, which can be helpful, but the drawback is that this requires less user input which can lead to inaccuracy in the analysis. Without Ansys this would not be possible to do in the timeframe of this project due to the complexity of setting up the mathematics and codes to run an analysis, so it is a fantastic tool that enables simulation of problems, but needs to be treated as a tool and not an engineer.

Multiple formulations exist today, and some examples are minimum potential energy, virtual displacements and mixed formulation between the two. Basic concept of minimum potential energy is that the deformation history does not matter, it is depending only on the initial and final displacements. The total potential energy contains the strain energy U or internal forces and the potential energy W, which are the external forces.

$$\Pi_p = U + W$$

Equation 9 Total potential energy [10]

A system that satisfy the equilibrium equations will give the stationary potential energy, and from the above formula the mathematical expression for minimum potential energy will prevail.

$$\frac{\partial \Pi_p}{\partial d_i} = 0 \, , i = 1,2, \dots, n$$

17

Equation 10 Minimum potential energy [10]

The next formulation is virtual displacement, also called virtual work, and states that for a body in equilibrium by small virtual displacements, the internal forces must be the same as the external forces on the body.

$$\int_V \bar{\epsilon}\, \tau\, dV = \int_V \overline{U}^T\, f^B\, dV + \int_{Sf} \overline{U}^{Sf^T}\, f^{St}\, dS + \sum_i \overline{U}^{iT}\, R_c^i$$

Equation 11 The principal of virtual displacement [10]

For the elements the use of minimum potential energy and virtual displacement can be used to obtain the relation between displacement and forces. A stiffness matrix must be created, and here the use of shape functions will appear. Those helps to describe the displacement field, and can be linear, quadratic or cubic. These choices will give us different ways of using the elements, if linear a much finer mesh will be needed to achieve good results. So, if a lot of elements is needed the solving time can increase.

If field quantities are defined and interpolated between points, this will not give exact answers but an approximation. The continuity of a field will also have different degrees. C^0 is continuous but not the derivative. C^1 is continuous and the derivative, but both are only this if the field quantity φ and the derivative are continuous. Beams and shells will often have C^1 but plane and solid bodies will often have C^0. And the field variable can be written on the form

$$\phi = \lfloor X \rfloor \{a\}$$

The relationship between nodal values $\{\phi_e\}$ and a_i will then be

$$\{\phi_e\} = [A]\{a\}$$

Equation 12 Relationship between nodal values and generalized d.o.f [10]

Then every row in $\lfloor X \rfloor$ and $[A]$ will be calculated at each nodal location. Further this gives us the relationship between the field variables and the nodal values and the formula for shape functions. The derivation of shape functions can be done in multiple ways, through solid mechanics and the relations existing here, but a polynomial function or a linear function will be needed to describe the deformation there also. The way presented here can perhaps be the easier way but demands more thinking or more work to really get the concepts. But through this we obtain

$$\phi = [N]\{\phi_e\} \text{ where } [N] = [X][A]^{-1}$$

Here the general equations are presented, and there can be seen that $\{\phi_e\}$ will be found when solving the global equations $[K]\{D\} = \{R\}$. Further the stress strain relationship will be shown, strain displacement relations and energy considerations. Not many elements can be generated using the direct method, and these relations mentioned above needs to be used. The stress-strain relations come from solid mechanics and are well known to most. Here strains and elastic constants will of course be implemented, and the zero subscript refers to initial stress, the stress-strain relation for linear elastic analysis will then become

$$\{\sigma\} = [E]\{\varepsilon\} + \{\sigma_0\} \ or \ \{\sigma\} = [E](\{\varepsilon\} - \{\varepsilon_0\})$$

Equation 14 Stress- strain relation [10]

To describe the strain-displacement relation, normal and shear strains will be used. And from this the strain field can be extracted through the partial derivatives of the displacement field. This comes from that the x-direction displacement u and y-direction displacement v are related through coordinates. In 3D also z-direction needs to be addressed, but the relations are shown below

$$\varepsilon_x = \frac{\partial u}{\partial x} \quad \varepsilon_y = \frac{\partial v}{\partial y} \quad \varepsilon_z = \frac{\partial w}{\partial z} \quad \gamma_{xy} = \frac{\partial u}{\partial y} + \frac{\partial v}{\partial y} \quad \gamma_{yz} = \frac{\partial v}{\partial z} + \frac{\partial w}{\partial y} \quad \gamma_{zx} = \frac{\partial w}{\partial x} + \frac{\partial u}{\partial z}$$

Equation 15 Strain relations [10]

This can also be set up in a matrix operator format

$$\begin{Bmatrix} \varepsilon_x \\ \vdots \\ \gamma_{zx} \end{Bmatrix} = \begin{bmatrix} \frac{\partial}{\partial x} & \cdots & 0 \\ \vdots & \ddots & \vdots \\ \frac{\partial}{\partial z} & \cdots & \frac{\partial}{\partial x} \end{bmatrix} \begin{Bmatrix} u \\ v \\ w \end{Bmatrix}$$

Equation 16 Strain matrix [10]

Relation between the strains is the compatibility, this must be satisfied in an isotropic material, like steel. And displacement-based finite elements which uses polynomials as displacement fields, will easily satisfy this condition.

Using the relation above to define how a stiffness matrix can be generated. The first, will be to relate the nodal displacements to the interpolation functions, then the strain-displacement matrix will be defined.

$$\{u\} = [N]\{d\}$$

The relation between how strains are related to displacements.

$$\{\varepsilon\} = [B]\{d\}$$

Where

$$[B] = [\partial][N]$$

Equation 17 B matrix formulation [10]

From the principal of virtual displacement, the relationship between stiffness, displacement and force comes into light. And since the energy put into a structure will give displacement, the virtual displacements show that the equilibrium will be satisfied. Therefore, the virtual displacements will below yield the other relations.

$$\{\partial d\}^T (\int [B]^T [E][B] dV \{d\} - \int [B]^T [E]\{\varepsilon_0\} dV + \int [B]^T \{\sigma_0\} dV - \int [N]^T \{F\} dV - \int [N]^T \{\Phi\} dS) = 0$$

This yield

$$[k]\{d\} = \{r_e\}$$

Then the element stiffness matrix is

$$[k] = \int [B]^T [E][B] dV$$

Stresses can then be evaluated from strain and the strain-displacement matrix

$$\{\sigma\} = [B]\{\varepsilon\}$$

Equation 18 Stress formulation [10]

4.2 Plasticity

The yield criterion that will be presented here is von Mises which represents isotropic hardening. This is a special part of the general plasticity theory and is illustrated with a representative schematic stress-strain diagram in figure 7.
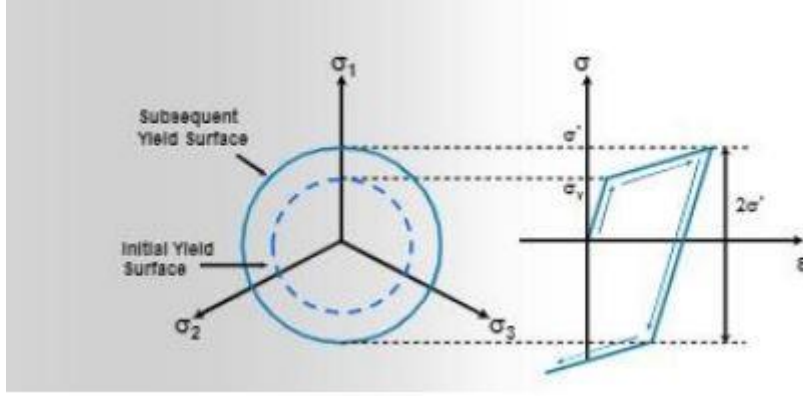
Figure 7 Yield surface, isotropic hardening

The isotropic hardening model is applied for the analyses done in this thesis, other yield criterion is also possible to use, since that will relate to the yield function. And the important stresses used in von Mises plasticity theory will now be the deviatoric stresses. And the von Mises stress will be checked against a value to determine if it satisfy the used material properties. Where the von Mises is presented with respect to deviatoric stress

$$\sigma_e = \sqrt{\frac{3}{2}} [S_x^2 + S_y^2 + S_z^2 + 2(S_{xy}^2 + S_{yz}^2 + S_{zx}^2)]^{\frac{1}{2}}$$

Equation 19 Von Mises [10]

The deviatoric stress will be the equal to actual shear stresses but the normal stresses with respect to deviatoric normal stresses will be the mean stress subtracted from the actual normal stress. The mean is then represented below

$$\sigma_m = \frac{\sigma_x + \sigma_y + \sigma_z}{3}$$

Further we need the plastic multiplier $d\lambda$, which are the effective plastic strain increment. The plastic modulus is needed H_p and P_λ, they are needed in the calculation of k_t and E_p. Where k_t represents the updated stiffness matrix and E_p the elasto-plastic stiffness matrix.

To calculate the plastic strain a forward, backward Euler scheme can be used, then an error check of the strain and stress. During these steps, elements need to be checked if they transit into plasticity or remain elastic. The hardening rule in this formulation will be the isotropic, and it could also be kinematic. It would not matter so much what one chooses due to that the analysis will only contain monotonic loading. This means that the unloading scenarios is not

21

present. One other important feature with von Mises plasticity is that the flow rule is associative. This implies that the flow is in the same direction as the yield surface normal.

$$F = Q$$

Where isotropic hardening gives

$$F = |\sigma| - \sigma_0$$

F will give a value that show if yielding and plastic flow is occurring then $F = 0$, below yield is not reached. And by differentiation of F with regards to σ for the different directions, since σ is related to the deviatoric stress. Then the E_p can be calculated as this

$$\left[E_p\right] = [E]([I] - \left[\frac{\partial F}{\partial \sigma}\right][P_\lambda])$$

The next part will be to update the stiffness matrix. This was a brief summary of the plasticity and in a finite element program with numerical method [10].

4.3 Solution procedures

In finite element when dealing with linear elasticity problem a direct sparse solver will be used. This will contribute to faster solving times and can variate from 2 to 15 times faster than a gauss elimination procedure. The symmetric condition of the matrix will give the opportunity to evaluate only the upper half. Using it with the skyline method only the nonzero terms needs to be evaluated. The recording of the equations also contributes to the efficiency of the sparse solver to minimize the fill ins when decomposition occurs, the two main recording schemes are minimum degree ordering and METIS ordering. With the use of Cholesky decomposition the equation that the direct sparse solver algorithm will begin to solve this equation below

$$[L][U]\{u\} = \{F\}$$

This procedure suits well for structural problems and when different element types are used together, like beam-shell. It is robust and does better with ill-condition matrix than the

iterative solver. But procedure requires a lot of memory and factoring of the matrix takes most of the time.

When rate-independent plasticity models are applied there is a need for a numerical method to be utilized with the direct solver. This can be the Newton-Raphson or the arc-length method. Here the load will be incrementally added, and the displacement found at each sampling point. This is because the load-deformation curve now is nonlinear, and the tangent stiffness must be updated at each sampling point to account for the plasticity. An error and residual force plot can be used to determine the accuracy of the method since this now will approximate the exact solution.

Newton-Raphson method is efficient and can converge relative fast. Different forms of the procedure can be chosen, like modified Newton-Raphson or full Newton-Raphson. The difference between those two is that full Newton-Raphson will calculate the tangent stiffness at each step, but the initial tangent stiffness can often be used for more than one step. When using the direct sparse solver, a new factorization will be done at each step and will often give longer solution time. When there is instability a method like arc-length method will be more beneficial. Because when the slope becomes negative of the load-displacement curve, the Newton-Raphson method will tend to diverge. This will often be a problem with Newton-Raphson method in a collapse or a buckling analysis, for example [10].
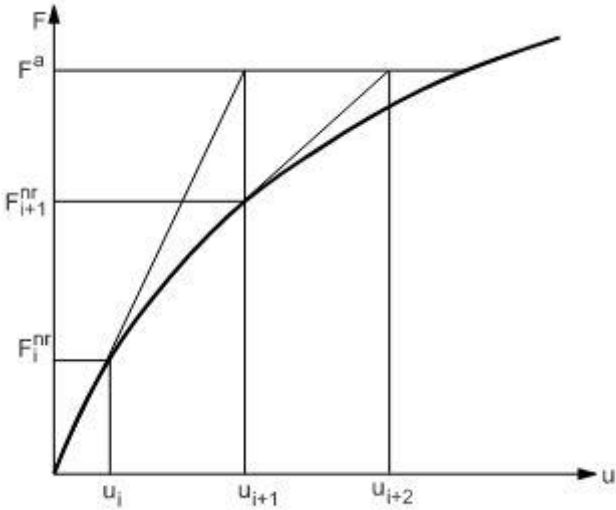
Figure 8 Newton-Raphson step [11]

23

4.4 Numerical integration

To be able to generate the stiffness matrix, numerical integration is the preferred method used in finite element method. This can be gauss quadrature, Simpsons rule, Newton-Cotes or other specialized rules. The gauss quadrature is widely applied and uses weighting factors and sampling points in the element to evaluate the field values. Special formulations are used for triangles and pyramids, solid quadratic elements use a 14 line rule. But for shell and beam elements the gauss quadrature procedure will mostly be used. When meshing with triangular shell elements a special form of the quadrature rule needs to be implemented to be able to achieve good results. The sampling points must be determined. This can be done through calculation, but it is easier to get them from the established table along with the weight factors. The gauss quadrature for three dimensions is presented below

$$I = \int_{-1}^{1} \int_{-1}^{1} \int_{-1}^{1} \phi(\xi,\eta,\zeta) d\xi d\eta d\zeta \approx \sum_{i} \sum_{j} \sum_{k} W_i W_j W_k \, \phi(\xi_i \eta_j \zeta_k)$$

Equation 23 Gauss quadrature [10]

Through this an approximation will be done, but the number of integration points can influence the answer. The complete integration does not necessarily give the correct element behaviour. This is very common for elements that experience bending behaviour, here a reduced integration will benefit to prohibit energy going to for example shear behaviour. There are given many recommendations in literature, for example [10].

The integration procedure take a more special form for triangular elements. A variable will appear in the integration limits and when evaluating the second gauss point the integrand will be multiplicated with a linear function. The formula below shows the evaluation of the element in the plane and not through thickness. The formula is presented in area coordinates as in [12]. The procedure of summation will be done according to what presented in the three-dimensional way.

$$I = \int_{0}^{1} \int_{0}^{1-L_1} \phi(L_1, L_2, L_3) \, dL_1 dL_2 \quad L_3 = 1 - L_1 - L_2$$

Equation 24 Gauss quadrature for triangle [12]

4.5 General element used

In structural analysis local- and global coordinate systems will be used, which is why local and global transformation is necessary. This is achieved with a transformation matrix. For

elements a Jacobian matrix will often be used to relate between referenced space to the actual space locally in the element [10]. These methods can transform different parameters to different coordinate system, which will be necessary for different postprocessing operations. A clear understanding of what coordinate system the data comes from can be crucial in the evaluation process.

4.5.1   Beam elements

First analysis will be done with beam elements based on the Timoshenko beam theory [11]. The beam deflections will be used to subtracted from the shell models to get net deflections. The use of beam elements are easier than shell elements, but still there are a lot of options (shape functions, mass matrix) that can give different results. An understanding of the element and analysis done, can improve the analysis. The beam elements will be straight, no curved formulations will apply here. The normal local coordinate system of a beam element are presented in Figure 9
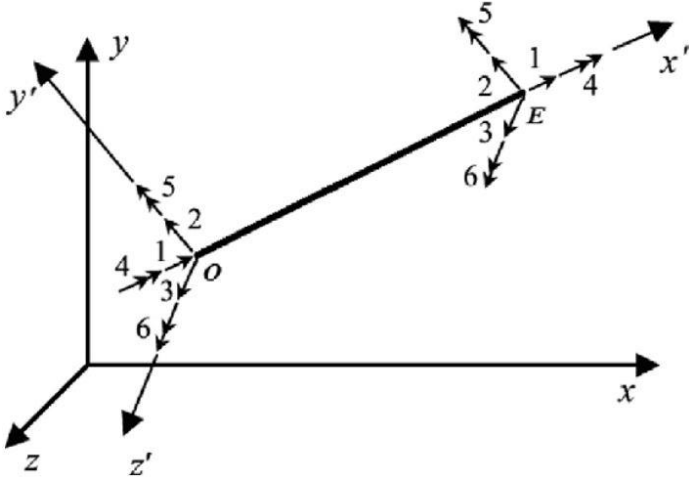
Figure 9 3D beam element

The Timoshenko beam considers the transverse shear component and is derived in the same manner as the Euler-Bernoulli beam. For the element stiffness matrix for the 12 DOF below it is assumed that z and y are the principal axes. This makes the cross section symmetric. But for a different cross section where these properties are not satisfied, new values will be needed in the stiffness matrix. Warping is not considered here, because this will not be a problem with the tubular joints for the thickness range in the analysis performed. Thin walled structures need this due to the torsion, then the element will get another two DOF's. The matrix in Figure 10 need a k factor for the transverse shear deformation, here accepted values needs to be used or lab test needs to be performed.

25

$$\begin{bmatrix} X & 0 & 0 & 0 & 0 & 0 & -X & 0 & 0 & 0 & 0 & 0 \\ & Y_1 & 0 & 0 & 0 & Y_2 & 0 & -Y_1 & 0 & 0 & 0 & Y_2 \\ & & Z_1 & 0 & -Z_2 & 0 & 0 & 0 & -Z_1 & 0 & -Z_2 & 0 \\ & & & S & 0 & 0 & 0 & 0 & 0 & -S & 0 & 0 \\ & & & & Z_3 & 0 & 0 & 0 & Z_2 & 0 & Z_4 & 0 \\ & & & & & Y_3 & 0 & -Y_2 & 0 & 0 & 0 & Y_4 \\ & & & & & & X & 0 & 0 & 0 & 0 & 0 \\ & & & & & & & Y_1 & 0 & 0 & 0 & -Y_2 \\ & & \text{symmetric} & & & & & & Z_1 & 0 & Z_2 & 0 \\ & & & & & & & & & S & 0 & 0 \\ & & & & & & & & & & Z_3 & 0 \\ & & & & & & & & & & & Y_3 \end{bmatrix} \begin{Bmatrix} u_1 \\ v_1 \\ w_1 \\ \theta_{x1} \\ \theta_{y1} \\ \theta_{z1} \\ u_2 \\ v_2 \\ w_2 \\ \theta_{x2} \\ \theta_{y2} \\ \theta_{z2} \end{Bmatrix}$$

[k] =

Figure 10 Beam stiffness matrix [10]

4.5.2 General shell elements

General shell elements are based on pure displacement formulation as beam elements. And then the shear and membrane locking must be removed in the formulation to prohibit too stiff elements. This is common for Mindlin-Reissner elements. And different methods to prevent this kind of behaviour could be integration scheme, formulation and number of nodes. Another check that should be done when using shell elements is that the formulation used will work for the thickness versus length ratio. Because the behaviour will change when thick and thin shell formulation is chosen. As an example, very thin behaviour would not account for the shear deformations and can often use the Kirchhoff plate theory.

To generate the shell element each node need a normal vector to generate the other node vectors. These other vectors need to be used to calculate the node rotations. The normal vector will often be calculated based on the corner node positions. Then the rest can be found by the cross product between the normal vector and a guiding vector. Shell will be calculated often in finite element software in the local coordinate system. There is a difference on isoparametric coordinates and the local system. The isoparametric does not give the physical element shape, for this the Jacobian are used to give the relation between these two. And the displacement for an arbitrary point in the element will be

$$\begin{Bmatrix} u \\ v \\ w \end{Bmatrix} = \sum N_i \begin{Bmatrix} u_i \\ v_i \\ w_i \end{Bmatrix} + \sum N_i \zeta \frac{t_i}{2} [\mu_i] \begin{Bmatrix} \alpha_i \\ \beta_i \end{Bmatrix}$$

Equation 25 Shell displacement for arbitrary point [10]

26

Further the strain-displacement matrix must be defined, this follows the procedure presented before.

$$\left[\varepsilon_x \ \varepsilon_y \ \varepsilon_z \ \gamma_{xy} \ \gamma_{yz} \ \gamma_{zx}\right]^T = [H]\left[u_{,x} \ u_{,y} \ u_{,z} \ v_{,x} \ ... \ w_{,z}\right]$$

Equation 26 Shell strain-displacment [10]

Next the Jacobian can be expressed like

$$x_{,\xi} = \sum N_{i,\xi}(x_i + \frac{\zeta t_i l_{3i}}{2})$$

$$x_{,\eta} = \sum N_{i,\eta}(x_i + \frac{\zeta t_i l_{3i}}{2})$$

$$x_{,\zeta} = \sum N_i(\frac{t_i l_{3i}}{2})$$

Equation 27 Jacobian formulation [10]

The next columns in the matrix will be similar. And from this the connection between the isoparametric coordinates and x,y and z.

$$\begin{Bmatrix} u_{,x} \\ u_{,y} \\ u_{,z} \\ v_{,x} \\ \vdots \\ w_{,z} \end{Bmatrix} = \begin{bmatrix} J^{-1} & 0 & 0 \\ 0 & J^{-1} & 0 \\ 0 & 0 & J^{-1} \end{bmatrix} \begin{Bmatrix} u_{,\xi} \\ u_{,\eta} \\ u_{,\zeta} \\ v_{,\xi} \\ \vdots \\ w_{,\zeta} \end{Bmatrix}$$

Equation 28 Isoparametric coordinates related to x,y,z [10]

From these formulations the B matrix is generated, then strain and stresses can be generated including the k stiffness matrix [10].

$$k = \int_{-1}^{1} \int_{-1}^{1} \int_{-1}^{1} [B]^T [E][B] det[J] d\xi d\eta d\zeta$$

Equation 29 Shell stiffness formulation [10]

When these shell elements are used with boundary conditions or elements are perpendicular to each other, the problem with a zero-stiffness mode can arise. To solve this a drilling dof can be taken into the element formulation or a penalty method can be used to prohibit this zero stiffness. This penalty method will give the in plane rotation a small stiffness to be able to

handle this. This will not give the element any ability to handle in plane torsion, but give the possibility to use it to connect to beam element or fixed boundary conditions etc [13].

$$k_T = \begin{bmatrix} k_{element\ 20x20} & 0 \\ 0 & kI_{4x4} \end{bmatrix}$$

Equation 30 Stiffness with six d.o.f penalty stiffness [13]

This approach does not always give the best results in nonlinear analysis, which is pointed out in [13]. This is due to local buckling and time stepping algorithm. But the code used by Ansys is not possible to open, so validation test will be done to be sure results are within reliable values. The best way is if the software can give the nodes five or six degrees of freedom when needed.

4.6 Ansys

The solver Ansys Mechanical uses are the same as in APDL, that is also what makes it powerful because of the APDL scripting language can be used to create parametric design [11]. The assumption then being that this language is known to the user, because the Mechanical graphical user interface allows for the implementation of commands to call different elements and keyoptions. To take advantage of these possibilities will certainly give the job of analysing multiple geometries much more efficient.

The isotropic material model as presented in the theory part is chosen together with a multilinear curve. The material chosen is steel grade S355, which is greatly used in load bearing structures both offshore and onshore. To generate the multilinear stress-strain curve the DNV-RP-C208 [14] was used. This gives an accepted curve used in the industry for material nonlinearity. For this application the engineering stress and strain can not be used, since this do not account for the change in area, then for Ansys the true stress(Cauchy) and logarithmic strain will be used [11].

$$\varepsilon_{true} = \ln\left(1 + \varepsilon_{eng}\right)$$

$$\sigma_{true} = \sigma_{eng}\left(1 + \varepsilon_{eng}\right)$$

Equation 31 True stress-strain [11]

Other material values presented here

Proposed properties for S355 steels (true stress strain)				
	S355			
Thickness [mm]	**t≤ 16**	**16< t ≤ 40**	**40< t ≤ 63**	**63< t ≤ 100**
E [MPa]	210000	210000	210000	210000
σ_{prop} **[MPa]**	320,0	311,0	301,9	284
σ_{yield} **[MPa]**	357,0	346,9	336,9	316,7
σ**yield2** [MPa]	366,1	355,9	345,7	323,8
ε**p_y1**	0,004	0,004	0,004	0,004
ε**p_y2**	0,015	0,015	0,015	0,015
K[MPa]	740	740	725	725
n	0,166	0,166	0,166	0,166
ν	0,3	0,3	0,3	0,3

To calculate the multilinear curve and implement it into Ansys, Matlab was used to create the material curves and then take points from Matlab table and plot them in Ansys. The elastic and the transition region are linear equations. But for the last curve in Figure 11 the formula presented below from DNV-RP-C208 [14] was used.

$$\sigma = K(\varepsilon_p + \left(\frac{\sigma_{yield_2}}{K}\right)^{\frac{1}{n}} - \varepsilon_{p_{y2}})^n$$

Equation 32 Material curve formula from DNV-RP-C208 [14]

This material model will not be valid after necking and can be used for ultimate strength but not for analysis of rupture. This will demand another type of material data and formulation.
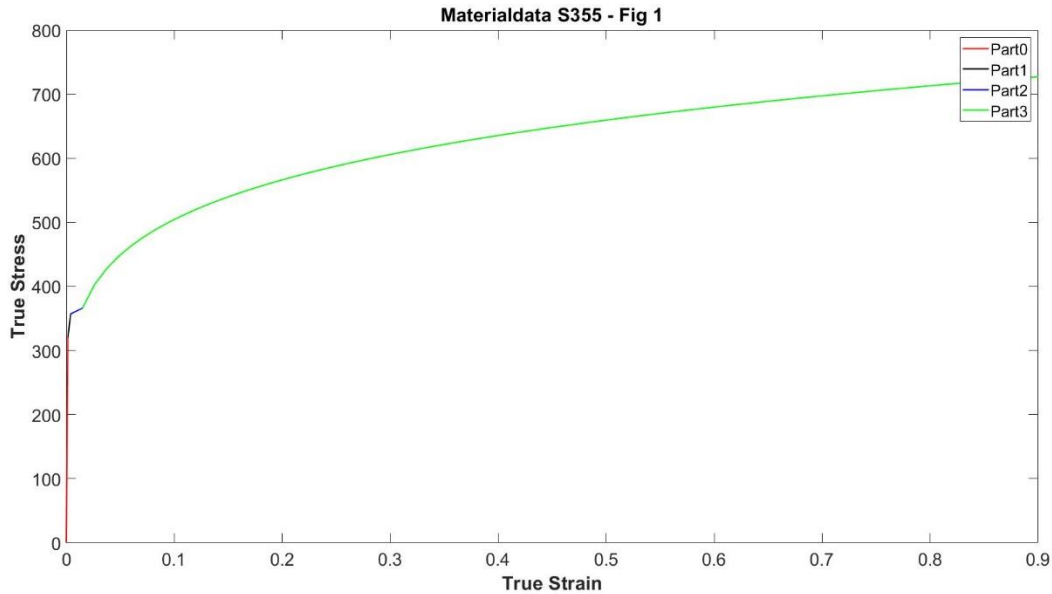
Figure 11 DNV-RP-C208 S355 material curve [14]

Modelling and geometry are done through Inventor and Ansys Designmodeler, this is to get the partitions that are necessary for the meshing algorithm. The need to get a systematic routed mesh is important for the result extraction. And to get mesh connection between different features modelled. Also, the modelling part must be done correct from the beginning due to what type of elements that is going to be implemented. For beams this will mean splitting up the lines to implement element to account for the distance between centre pipe to outerwall. For the shell the direction of the local coordinate system will be important for post processing.

Meshing in Ansys will be done with Beam189, MPC184, Shell281, Solid186 and Solid187. The beam element will have three integration points in the axial direction and use numerical integration also to calculate the cross-section properties. The integration points in the cross section will often be 2x2 at each section, because it will get split up into pieces. For the shell elements a 2x2 and 5 integration points through the thickness [11]. This can also be seen to be chosen in DNV-RP-C208 [14]. For the solid elements reduced integration are chosen, but then more than one element through thickness must be used. And all the elements have been chosen to use quadratic interpolation functions. For most of the models the shell281 element will be used. And this element has an advanced formulation for the curvature and uses a penalty method for the drilling stiffness. It is also well suited for analysing elastoplastic behaviour with thin to moderately thick shells. This element will be used as triangles and

rectangular, the triangles will have a six node configuration and the rectangular an eight node configuration.

For loading and restraint of the tubular joint a multipoint constraint and named selection will be used. This connects nodes on edges and vertices to the load. These are strong tools when it comes to analysis where repeatability comes into play. All the joints will have fixed ends at the chord.

The sparse direct solver is used and the Newton-Raphson solution scheme and large deflection (NLGEOM) is on for nonlinear analysis. NLGEOM activates the large strain and large rotation. Time stepping algorithm can be set to auto to take advantage of faster convergence. Time stepping in the analysis is not real time but fictious time used to subdivide the load, because the applied load must be added in steps due to numerical methods.

4.7 Regression

Regression method will be used to fit generated data to a function. The data will be implemented as a matrix of variables. The most reasonable approach is to limit the number of variables as much as possible. The method used is a nonlinear least square. The variables change in a nonlinear way which is way you need a nonlinear algorithm. Linear regression will give poor fit estimations because it cannot fit an exponential function or a polynomial function, or other higher order functions. The mathematical background presented below can be read in more detail [15].

With the known function and the response(x,y), the regression expression becomes the form presented below.

$$y_{ij} = f_j(x_i; \theta^*) + \epsilon_i \ (i = (1,2, \ldots \ldots, n, \quad j = (1,2, \ldots \ldots, n))$$

Equation 33 Regression function [15]

From the expression above minimizing of the square sum of the coefficients(θ).

$$S(\theta) = \sum_{i=1}^{n} [y_i - f_i(\theta)]^2$$

Equation 34 Square sum [15]

The most common way to express the minimization problem is in form of a Hessian matrix and a gradient of S(θ). The Hessian matrix can be expressed as

31

$$H(\theta) = \frac{\partial S(\theta)}{\partial \theta \partial \theta'} = 2(J'J + A)$$

Finding the derivatives and an approximate the Hessian matrix will be important for all the methods and the Gauss-Newton method assumes that this is possible with only first derivatives. And the rank of the matrix will give some indication on how the Gauss-Newton method will work. When Jacobian is not of full rank the algorithm can perform poorly. When this happens, the Hessian matrix will have a poor approximation, and the solution is no longer unique. Also, the Gauss-Newton assumes that A(θ) is small compared to J´J. This will be one weakness of the algorithm because of divergence.

$$\theta^{(a+1)} = \theta^{(a)} + \delta^{(a)}$$

Formula above is formulated from the Newton algorithm and is the Gauss-Newton step. For the full explanation referred to [17]. In Matlab the Levenberg-Marquette algorithm is used and this has changes related to the $\delta^{(a)}$.

$$\delta^{(a)} = -(J^{(a)'}J^{(a)} + \eta^{(a)}D^{(a)})^{-1}J^{(a)'}r^{(a)}$$

But more recent methods for computing the $J^{(a)'}J^{(a)}$ exists and are based on calculating $\delta^{(a)}$ as a linear least square problem.

$$\underset{\delta}{Minimize} \left\| \begin{pmatrix} r^{(a)} \\ 0 \end{pmatrix} + \begin{pmatrix} J^{(a)} \\ (\eta^{(a)}D^{(a)})^{0,5} \end{pmatrix} \delta \right\|^2$$

The methods used are gradient based and Newton based. Some algorithms will take advantage of this, and both methods will be implemented, and it will interpolate between the step directions. The Gauss-Newton algorithm has been altered to the Levenberg Marquette to be able to handle problems with ill-conditioned and singular matrices by changing the Gauss-Newton step. The Levenberg Marquette also implements a full trust region method and line search has been added to the algorithm. The main goal is to get a reliable and not time-consuming algorithm. In the multivariable regression analysis, the x and y will be

implemented in matrix form. In the regression an initial guess on the prediction coefficients are needed, and here a guess as close as possible to the solution will prevent the algorithm to diverge.

5 Validation

5.1 Shell and former research

First model to be created was a beam model in Ansys. This was necessary for extraction of the net deflection of the shell models and the solid model. The choice of input parameters was taken from the MSL study [4] on the shell platform where values from the SACS with Buitrago's flex element is used. The model values here will be used and the validation will be done against Buitrago and other earlier research.

Table 2 Validation geometry data from [4]

Validation Parameters								
Specimen No.	Loading Type	Geometry	D (mm)	d (mm)	T (mm)	t (mm)	Load (kN,kNm)	Chord Wall deformation (rad,mm) Buitrago Flex elem.
TM-39	IPB	T-joint	355,4	317,4	15,1	8,7	405	0,0093
TM-2	OPB	T-joint	216,45	165,55	4,5	4,53	6,8	0,0177
TC-12	Axial	T-joint	318,5	139,8	4,5	4,4	76,5	2,241

From Table 2 the models were built, and length of chord was set to 1500 mm and brace set to 500 mm from centre chord. If one of these lengths are too short, it can give incorrect results due to boundary condition influencing the chord wall deformation. The results were extracted at the brace end of the beam models. Then these will be used to subtract from the deformation taken from the shell or solid model. The representation of how the beam models were built in Ansys can be seen in Figure 12. In Figure 12 there are no elements between chord and brace. This intersection is modelled with a mpc184 element to achieve the empty space in the pipe from outer wall to centreline. This is implemented by using APDL commands into mechanical.
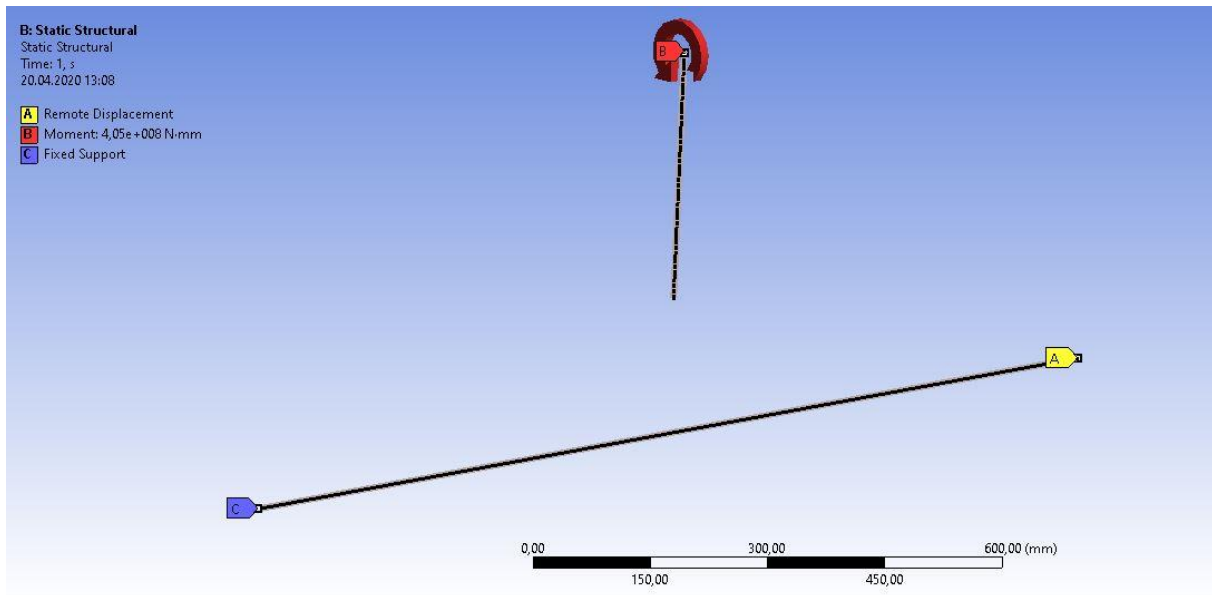
Figure 12 Ansys beam model

In Ansys extraction of the results can be exported to excel and then be processed in Matlab to generate graphs. And for comparison the equations from Buitrago [9], Fessler, Efthymiou [8] and MSL [3] are calculated through Matlab. Then a comparison between the Ansys and their equations can be done. To generate the comparison the beam model results will be essential and are presented in Table 3. These will be used to subtract the beam deformations from the shell models or solid model.

Table 3 Ansys beam model results

Beam model results					
Specimen No.	Loading Type	Geometr y	Load (kn,kNm)	Brace End Deformation (rad,mm)	Chord Deformation (rad,mm)
TM-39	IPB	T-joint	405	0,0076304	0,001438
TM-2	OPB	T-joint	6,8	0,0023467	0,00093971
TC-12	Axial	T-joint	76,5	0,3403	0,2775

Research on tubular joints have been done either by shell or solid. Solid will give more difficulty when it comes to do a design of experiments (doe). This comes from the number of elements needed and hence the solving time for each case will be enhanced drastically. To achieve a reliable and efficient model that can be solved fast and give accurate results, the shell has many of these features. To verify that it will perform for the tubular joint a test against the earlier accepted equations and solid will be presented. The shell model created in

34

Ansys for the test are presented in Figure 13. Here multiple instances are created to control the meshing, this will also be done for the parametric models. To keep track of the quality and factors related to the elements, Ansys offers a tool called mesh metrics.
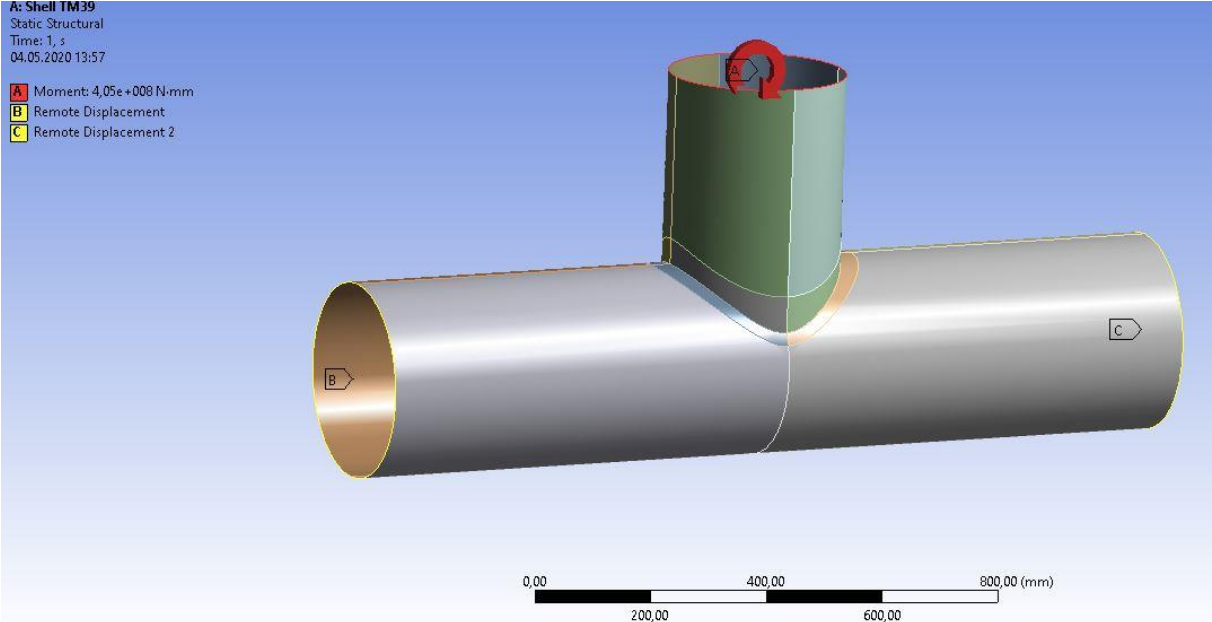
Figure 13 Ansys shell model

All the shell models used for the validation, except the weld model, uses the midsurface. But for the shell including weld effects the chord uses chord outer surface while the brace has midsurface. In Figure 14 the axial comparison between shell and the established equations have been done. Here the Ansys model is linear and the MSL nonlinear equation is included for comparing of the linear part and to look how the curve compares against the linear equations. The reason for expressing tension in the MSL nonlinear is due to that in MSL the axial loading is divided into compression and tension [3].

35
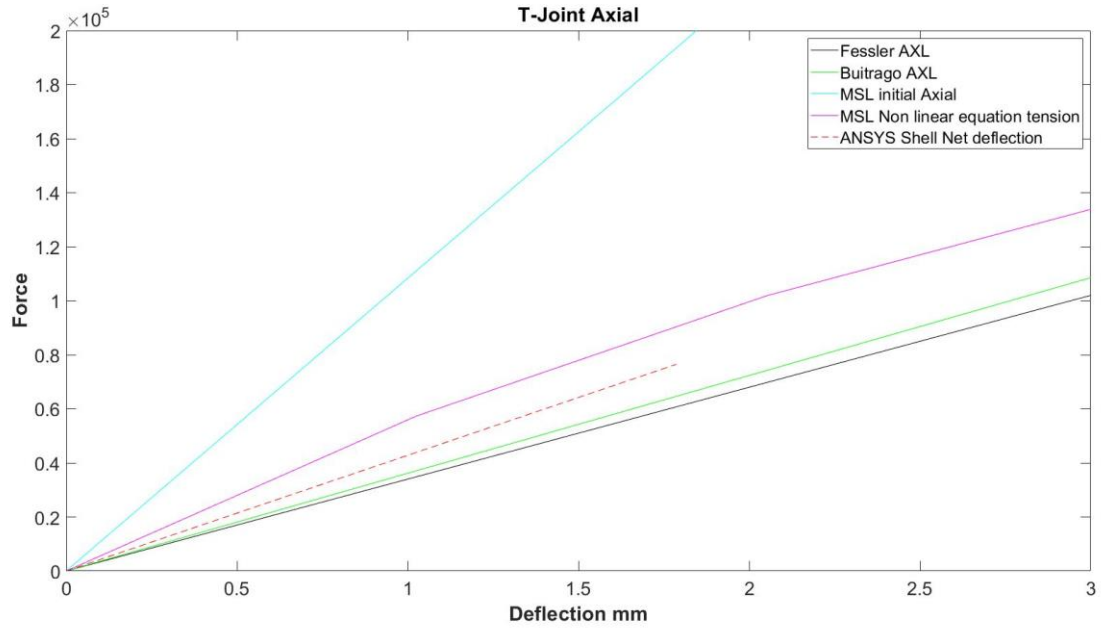
Figure 14 TC-12 with axial loading

Figure 14 show that the MSL initial stiffness (blue) [3] is much higher than the other ones. There is also some difference between the Ansys (dotted line), Buitrago [9] and Fessler [8]. These give a softer behaviour than MSL, but their equations do not account for that the load is in tension or compression, which can be a reason for the softer structure. This indicates a good relation between the Ansys shell model and the equations. To validate the shell model further a database with multiple experiments will be needed.

In Figure 15 the in plane bending has been done, and the results shows agreement between Ansys shell and the equations. But the MSL nonlinear equation [3] curve seems to be too soft. The reason for this can be that the MSL equation do not predict the response well enough when beta gets close to 1. This will be tested with a full nonlinear comparison between the MSL equation against models presented in the MSL study [3].
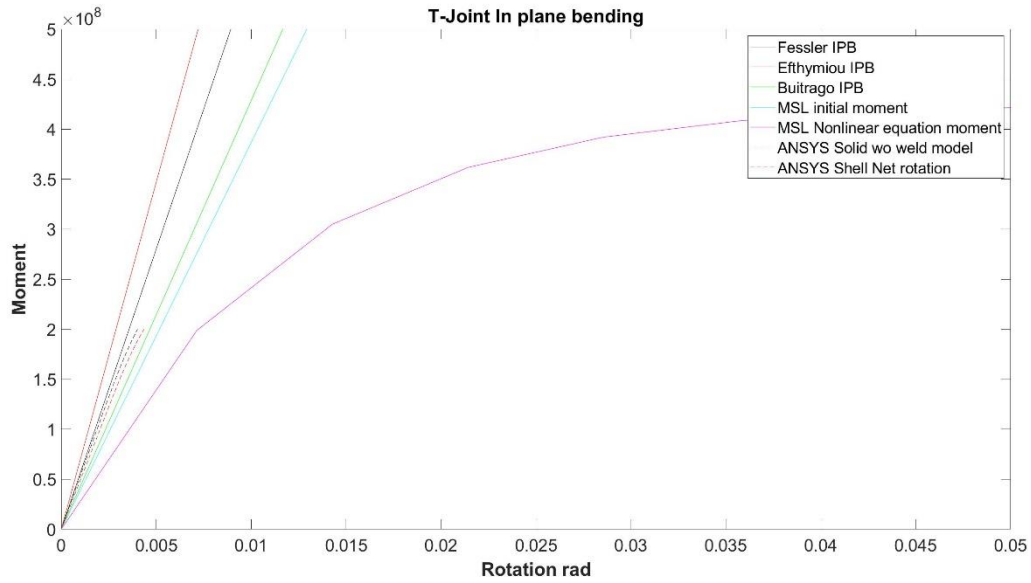
Figure 15 TM-39 with in plane bending

The out of plane bending was compared against the earlier equations and are presented in Figure 16. Here the shell model results also show agreement with the equations. Ansys shell follows Efthymiou (red) [8] prediction, and the MSL [3] equation does not perform better for this case. The MSL equations [3] aims to give the capacity and the force-displacement curve, but that the initial stiffness is inaccurate can lead to poor predicted deformation results for certain joints. Since the initial stiffness is implemented in the nonlinear MSL equation [3], there would be expected a closer relationship between the initial MSL stiffness [3] and the linear part of the nonlinear MSL equation [3].
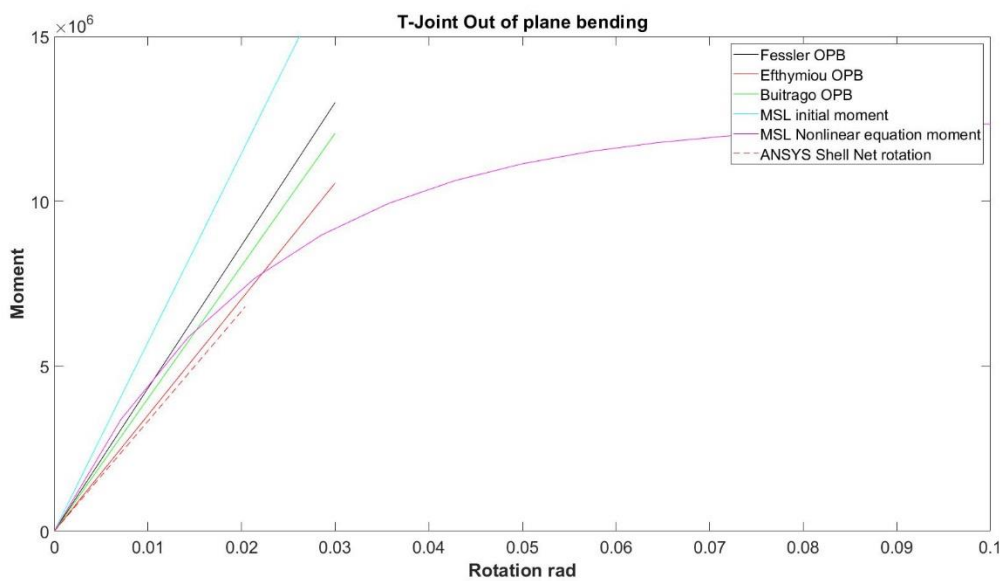
Figure 16 TM-2 with out of plane bending

37

Differences can be seen in all the equations, and their performance changes from load type to what the geometrical values are. When using these equations, the difference between calculated and experimental results can be larger than expected. But since the joints are used in a frame and here partial factors are used, these uncertainties in the joint behaviour could be accounted for in the partial factors. MSL does this for the nonlinear capacity by giving a characteristic load [3]. As for the tests performed against the shell model, it can be concluded that the shell model will perform satisfactorily. Because the results corresponds with the different equations.

5.2 Shell and solid

Next a comparison between solid and shell will be performed. An acceptable criterion is that a difference in results must be less than ten percent. Over ten percent in difference will not give confidence in the results achieved by the shell modelling. The difference between shell and solid should be quite small. This is controlled by comparing stress and deflection. A mesh sensitivity study was done to compare the stress and change in results due to mesh size. The results are presented in Table 4.

Table 4 Shell and solid comparison results

Shell			Mesh				Solid			
Deflection [mm]	Stress [MPa]	Elements	Shell		Solid		Deflection [mm]	Stress [MPa]	Elements	Percent diff.
2,4775	359,85	29017	10	5	10	5	2,3896	358,39	139158	3,547
2,4762	360,62	103187	5	2,5	10	4	2,3941	358,14	224452	3,315
2,4753	360,5	160360	4	2	15	3	2,3969	358,58	370555	3,167
-	-	-	-	-	-	-	-	-	-	3,462

Stresses were retrieved from chord on crown, the deflection was taken as the directional deformation in the remote point where the in plane moment was added to the brace. The geometry used in the test was TM-39, and the stress extraction was done by choosing the node that lies at approximate distance given in DNV-RP-C203 [16]. The stress is unaveraged and extrapolated using quadratic function from the integration point in the element. The stress used are Von Mises for comparing stresses. If the goal is to understand better how stress flow in the structure, normal stress in the local element coordinate system would be more beneficial. But these are only stresses compared against each other, if they are taken from the

same distance from the intersection this should give reliable results for comparison. The percentage difference in Table 4 shows that the shell model performs satisfactorily. The percentage are calculated from the deflection since this is the important value for the calculation of flexibility, and the difference in percentage between minimum solid elements and maximum shell elements are calculated. Still the difference are just above three percent, which gives good confidence that shell is a good way to model these joints. In Figure 17 the solid model is shown. The different elements and shapes can be seen, since reduced integration is used here, more than one element through thickness will give best results due to bending stiffness.
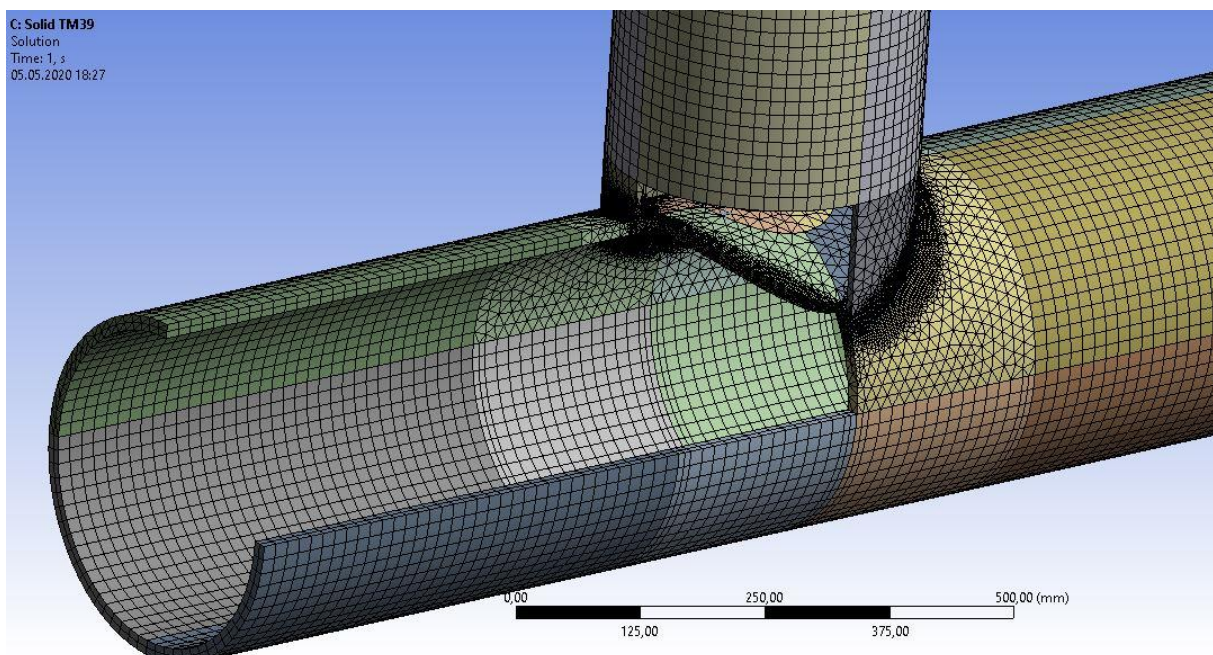
Figure 17 Ansys solid model

5.3 MSL nonlinear equations

Further the nonlinear test against MSL equations was done. Here geometry was taken from MSL2000 report [3], this was due to that MSL equation did poor on predicting the response in the linear test cases. In Table 5 the geometry is presented, those are collected from MSL2000 report. These have also been tested in the MSL2000 rapport with Abaqus against the MSL nonlinear equation from the report [3]. MSL gives very poor description of how they have measured their results and gives room for misinterpretation.

Ansys shell models were created to compare against the capacity and deformation curves. In the analysis settings for the nonlinear shell models, large deformation is on, line search and Newton Raphson type is chosen by the software and auto time stepping is on. This setup gives

39

fast convergence and seems reliable. This can also be seen in the in plane bending case where the model was run until nonlinear ultimate load, which gives some information that numerically the model is stable.

Table 5 Validation geometry data from [3]

Loading Type	Geometry	D(mm)	d(mm)	T(mm)	t(mm)	Length Chord	Length Brace
IPB	DT	1020,4	408,164	20,4	16,524	8163,2	1500
AXL	T	1020,4	408,164	20,4	16,524	8163,2	1500

The mesh in a nonlinear finite element analysis is more important than in a linear structure. This is because the solver will stop if elements get highly distorted. These requirements can be adjusted by element quality, restrictions in element shape or birth/death of element. And when using the shell281 element one should avoid triangular elements where strain gradients are high. Here the quad8 elements should be used and not the tri6 elements, tri6 should only be used as "filler" elements [11]. In Figure 18 the mesh of the DT-joint is presented, and here a mapped meshing is used in the joint intersection.
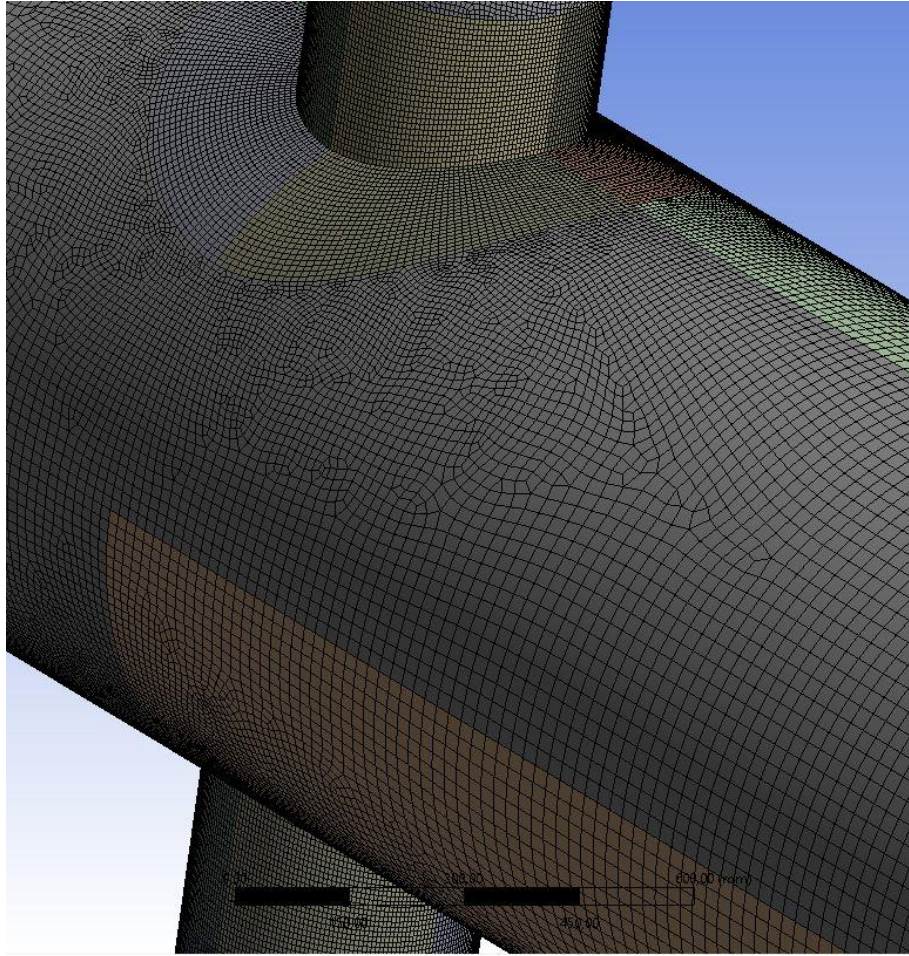
Figure 18 Ansys shell DT-joint

As seen in Figure 19 one problem that will occur when using these type of shell models is when large strain occurs, because elements in the intersection will experience large amount of strain. This will not necessarily reflect the real strain at this point, because the weld will have another stiffness and geometry in the real joint. That is why it will be difficult to establish for example fracture of the joint with regards to strain in these models.
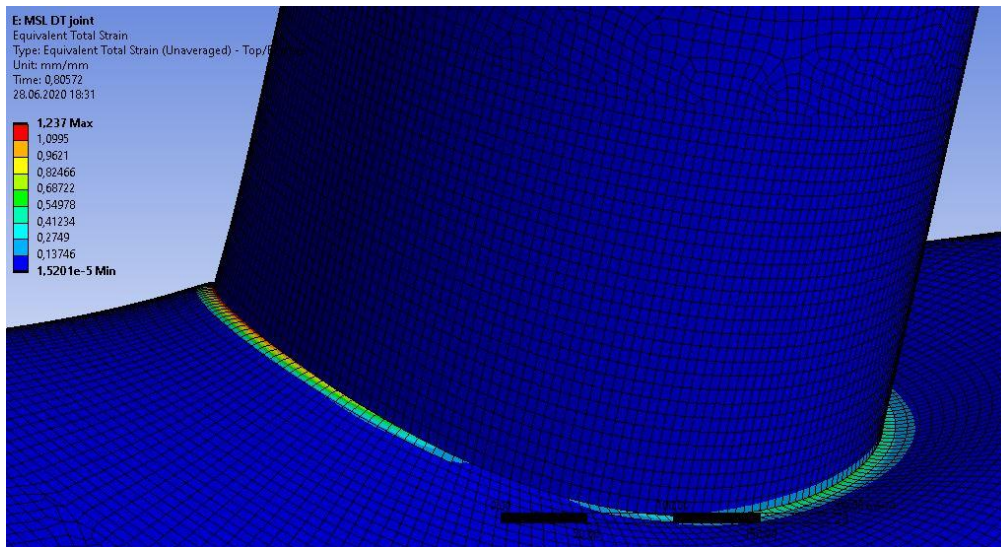
Figure 19 DT-MSL2000 joint [3] equivalent total strain at time 0.8

The main task will be to get the joint to behave according to the earlier research done by MSL, this will be to check the load deformation curves. If this should be used in a code or standard, a form of deformation limit should be established. MSL do have it for axial deformation but not for the moment [3], so to establish a limit experimental work needs to be done together with more extensive finite element modelling. In Figure 20 the total equivalent mechanical strain and moment are presented against the intersection rotation. The strain can be seen to be very high at the intersection between chord and brace, which gives a problem in defining the ultimate load due to strain. Other software related for example EN-3 code [17] uses five percent plastic strain to give the ultimate load and in a tensile test the rupture occurs at between fifteen to twenty percent strain.
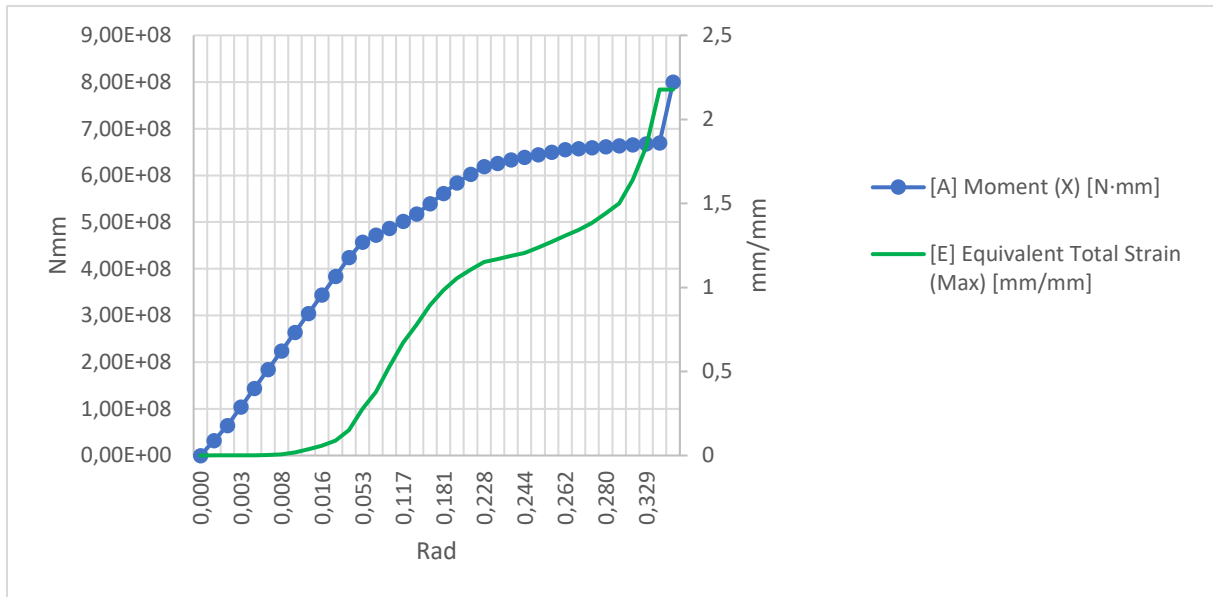
Figure 20 Moment versus strain in DT-joint

Comparison plot, Figure 21, between MSL equation [3] for the in plane bending case and the finite element model with shell281 seems to fit good, the shell model gives a higher load before instability occurs in the model. The overall performance gives good indication about the response of this DT-joint.
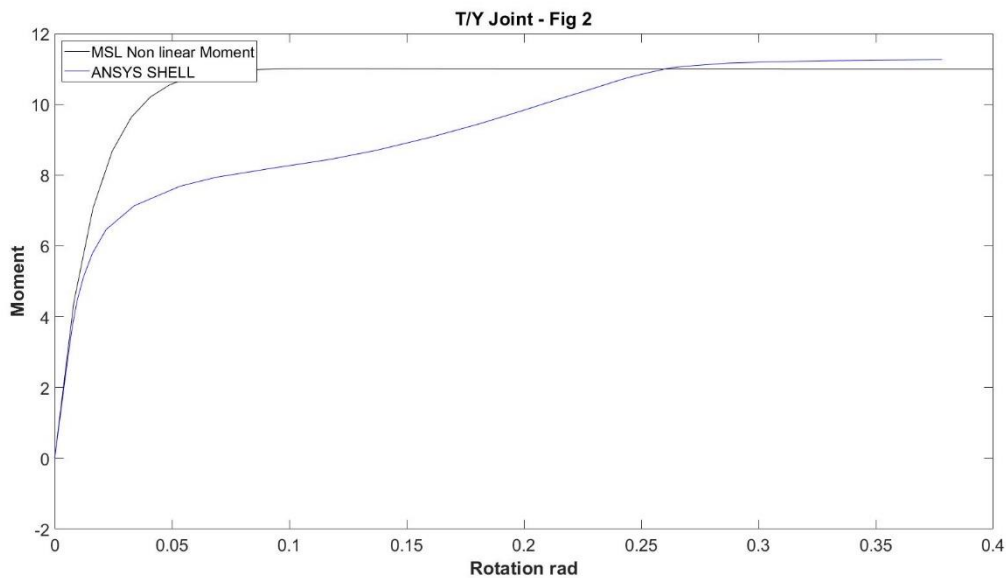
Figure 21 Moment-rotation for DT-joint

Further the axial deformation plot between MSL nonlinear equation for and finite element is presented in Figure 22, and here agreement between both can be seen. But as seen in the validation with the linear equations, MSL seems to have some spots in the validity range where the response deviates to some degree. This can come from number of reasons, from

43

extraction of results and FEA analysis to that a part of the research also depends on frame test. Especially when the deformation are large differences occurs in the axial loading. Here the shell model gets stiffer, but it is important to keep in mind that when MSL [3] did their analysis they excluded hardening model. How much this affects the analysis is difficult to guess, MSL [3] concluded that the effects are small. Some problems also arise with the elements in the axial case and refinement of the elements and reduced stabilization based on energy was set on in the analysis. The stabilization values were taken from [18] and as a recommended test the stabilization energy should not be larger than 10 percent of the strain energy. But the most efficient way to get convergence was to refine mesh and get elements in the chord-brace intersection, where high strains occur, to be perfectly squared.
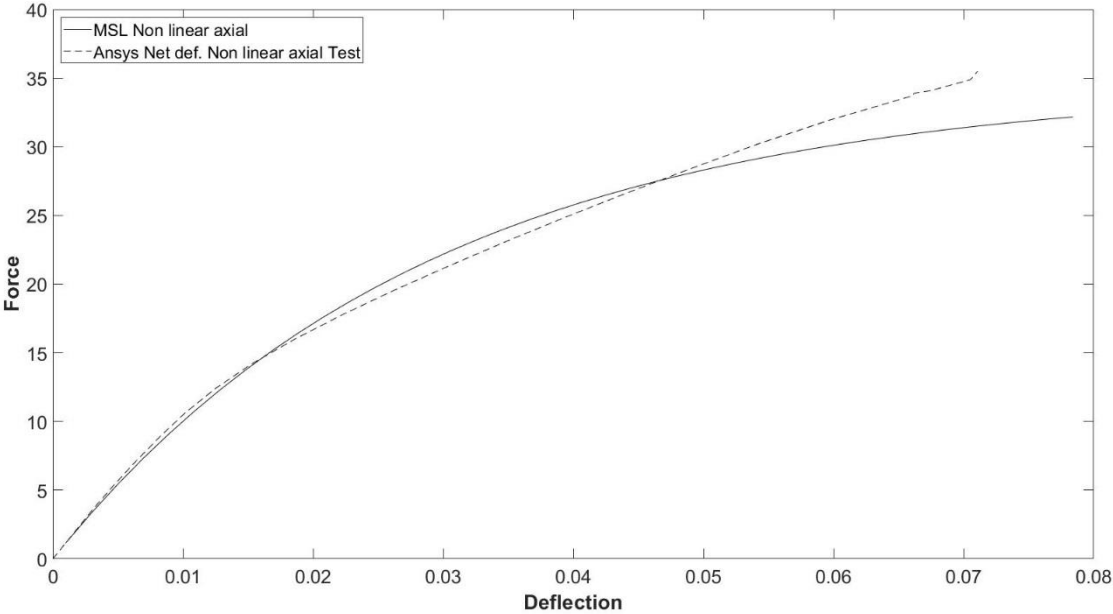
Figure 22 Force-deflection for T-joint

5.4 Weld in shell

MSL [3] rapport concludes that welds are not necessary to be accounted for, this can be correct for the way displacement are collected by Buitrago [9]. But the local effects in the chord, when it comes to strain and displacement, can have poor relation to real tests. This is also in a way presented in the DNV-RP-C203 [16] standard where stresses are collected at a distance from the intersection to give more correct results. From the MSL2000 [3] rapport there are commented that for joints without weld, strain is not a good way to predict failure.

Comparison was done between a shell model of the TM-39 with and without weld, paths were created in Ansys to track the different deflection and element stresses. When doing these

types of comparison with stresses, results need to be picked at the same point or surface in each model. Since shell have a top, mid and a bottom surface. There will be important to report stresses at correct surface or same point in the shell models. In Ansys element triads can be used to ensure that the correct results are collected. Element triads are the same as element local coordinate system, the global and the local are shown in Figure 23.
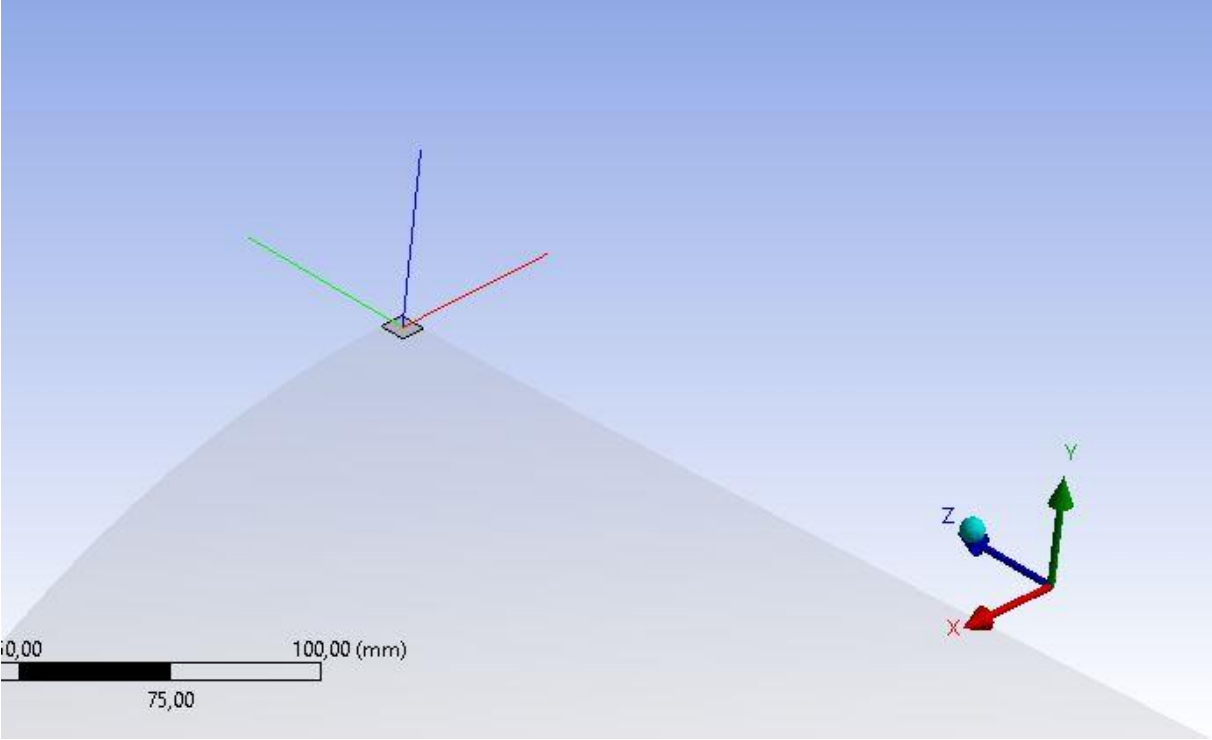
Figure 23 Local element coordinate system and global coordinate system

Paths and how the extraction of the results are done is shown in Figure 24. The paths are construction geometry in ANSYS and to ensure that the correct results are taken out, an option is to connect them to related nodes. Also, to get the element results in accordance with the local element coordinate system, the solution coordinate system must be specified, or else the results are transformed into the global coordinate system. Since the weld toe will not start at the same location in the models, the path will begin at the intersection between brace and chord and at the weld toe in the model with weld.

45
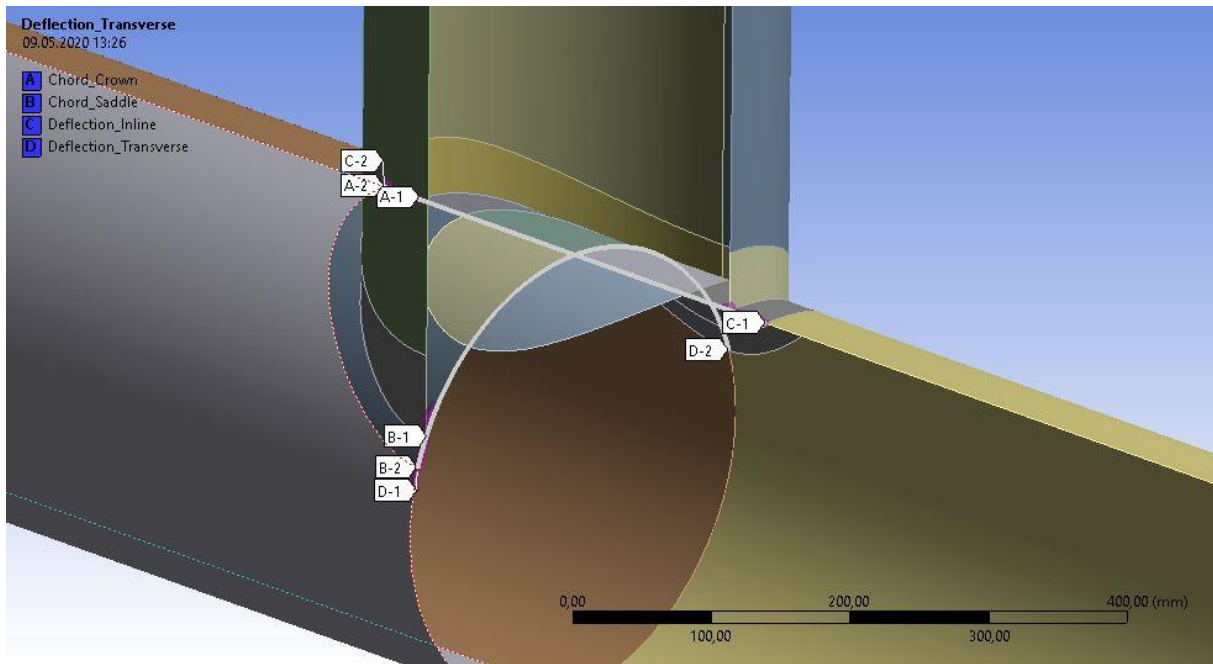
Figure 24 Path in shell model to extract output

The weld will change geometry from the saddle to the crown, and to get a weld that fits with weld practice, the geometry was taken from Figure 25. The shell model was split up into 15 instances, and the geometry was drawn at each instance to get a smooth transition. All the geometry was done in Inventor then transferred into designmodeler in ANSYS for further cad work and clean-up.
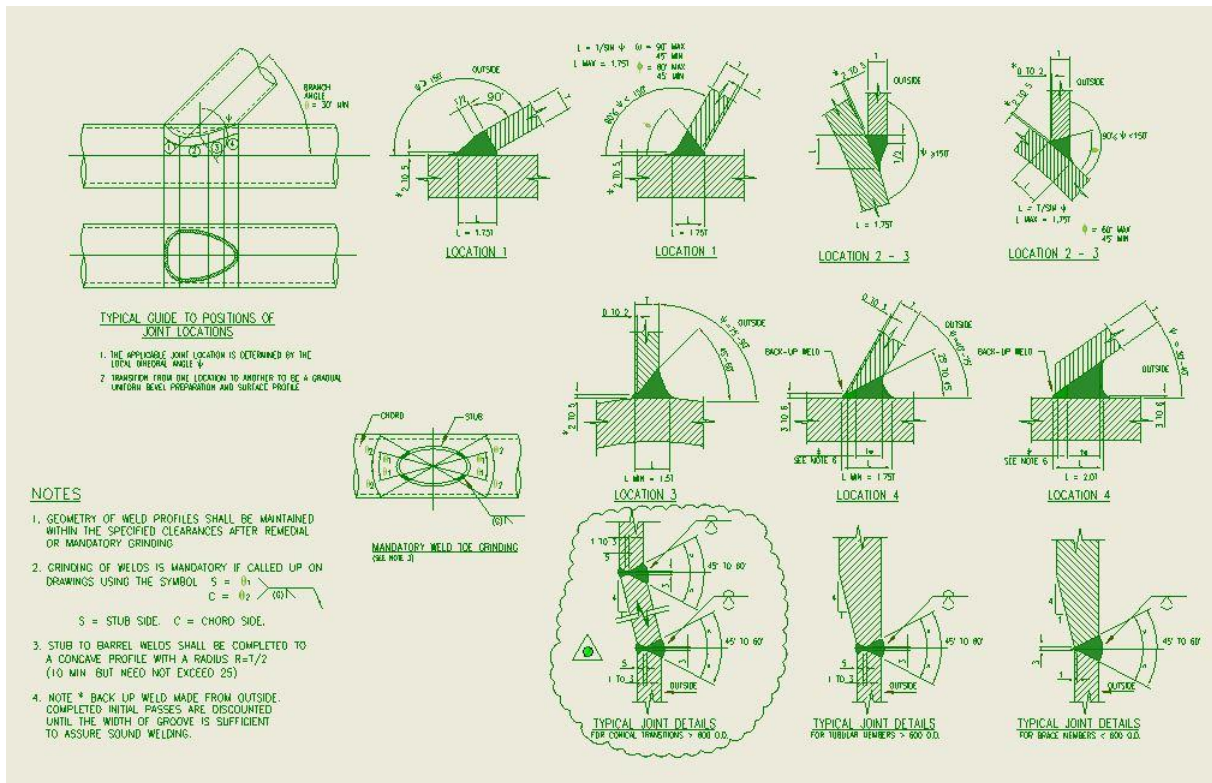
Figure 25 Weld configuration

The work with modelling a weld is time-consuming, especially with a solid model, since the partitioning and to capture how the weld changes from saddle to crown. To do this work when doing a parametric study would be as just stated, time-consuming, and will not necessarily give more accurate results when it comes to flexibility, but sometimes it is important when analysis involve results where the weld inflict those results. But that must be a judgment done by the engineer, but if not necessary these test shows that the difference in deflection is very small. From these paths presented in Figure 24, all the results were taken into graphs for comparison. The results on the model without weld is taken from chord-brace intersection and on the model with weld at the chord weld toe. In Figure 26 the mesh and implemented geometry are shown as a cut through the model in Ansys, and the weld changes angle from saddle to crown to represent the weld presented in Figure 25. Meshing has been refined in the weld area to have a uniform mesh to extract results from.
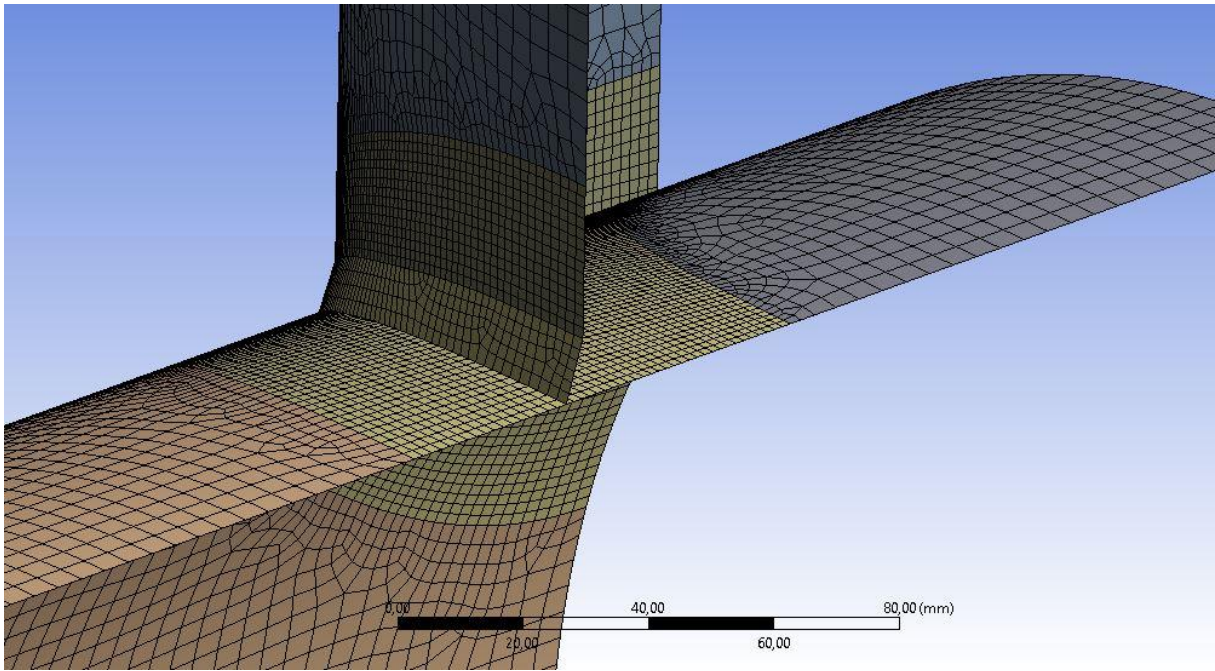
Figure 26 Shell weld model
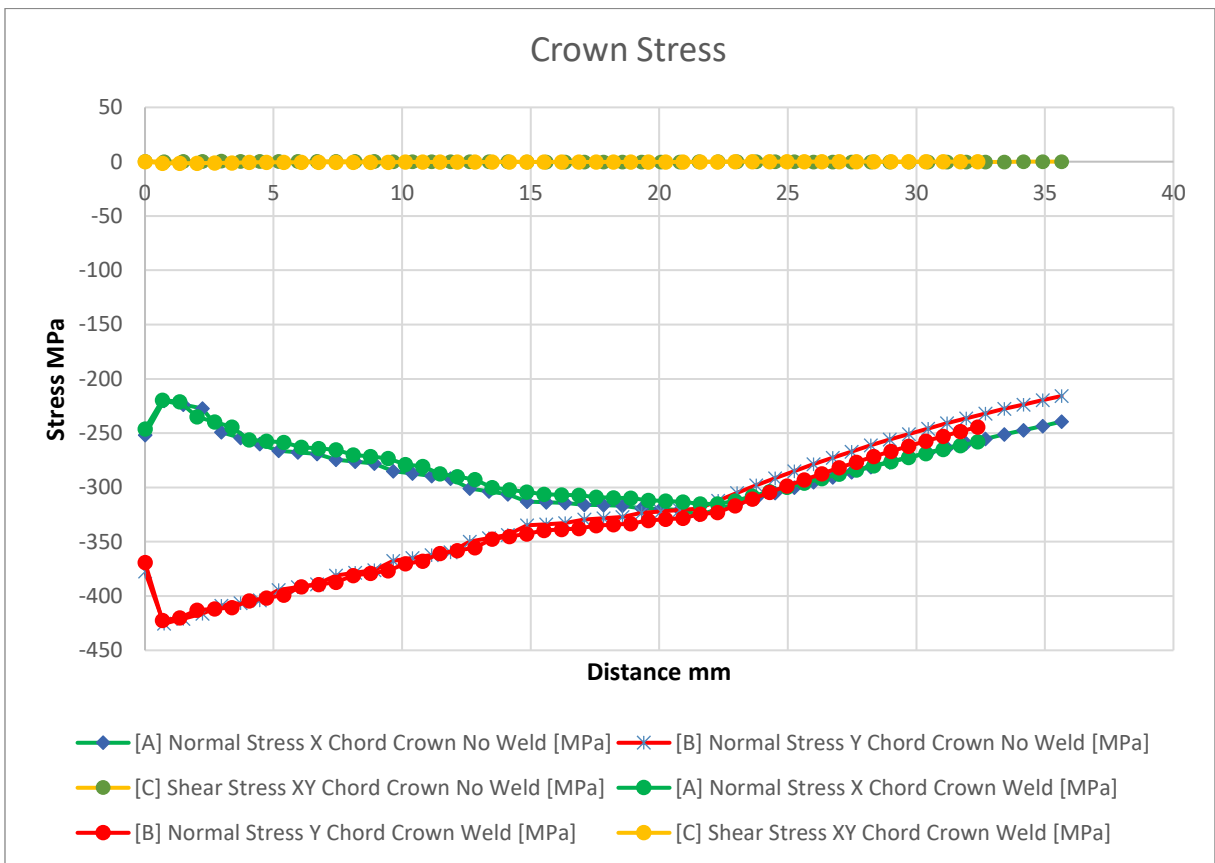
Figure 27 Element normal stress chord crown
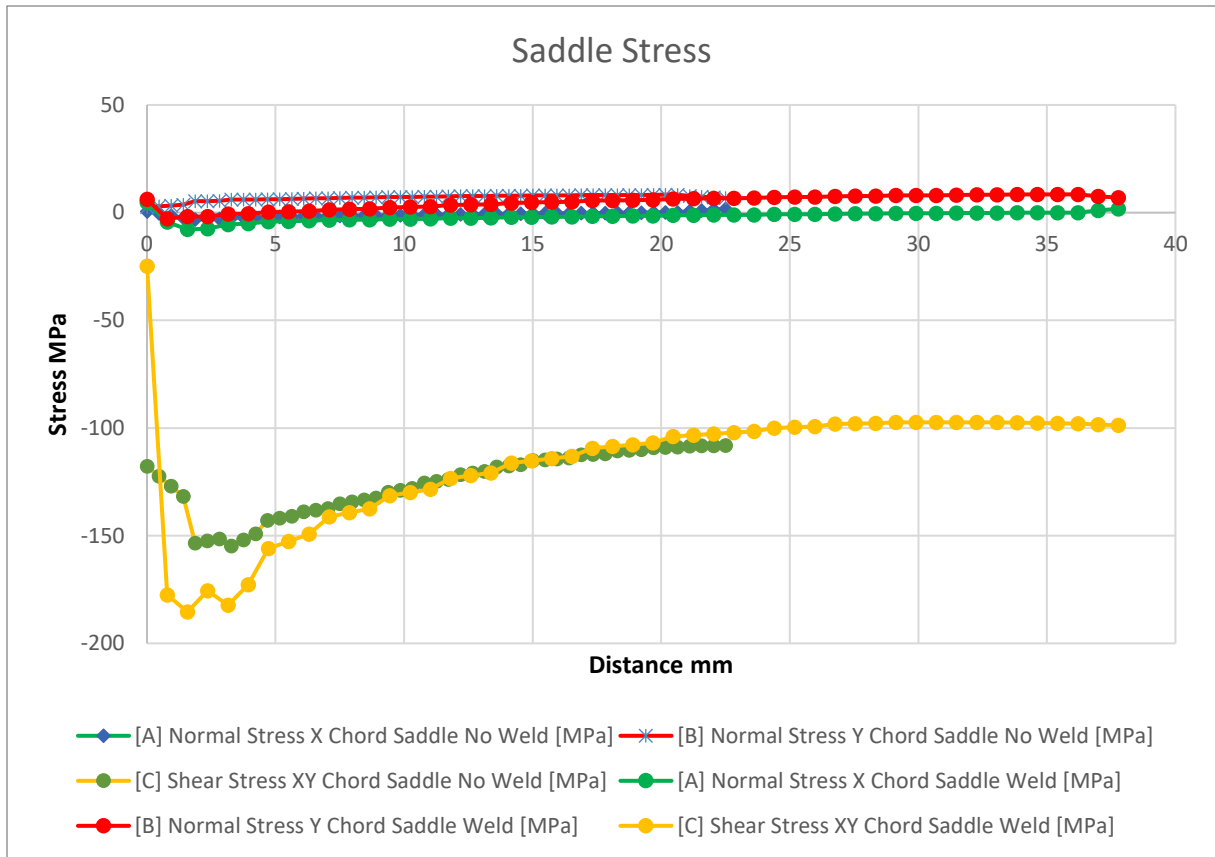
Figure 28 Element normal stress chord saddle
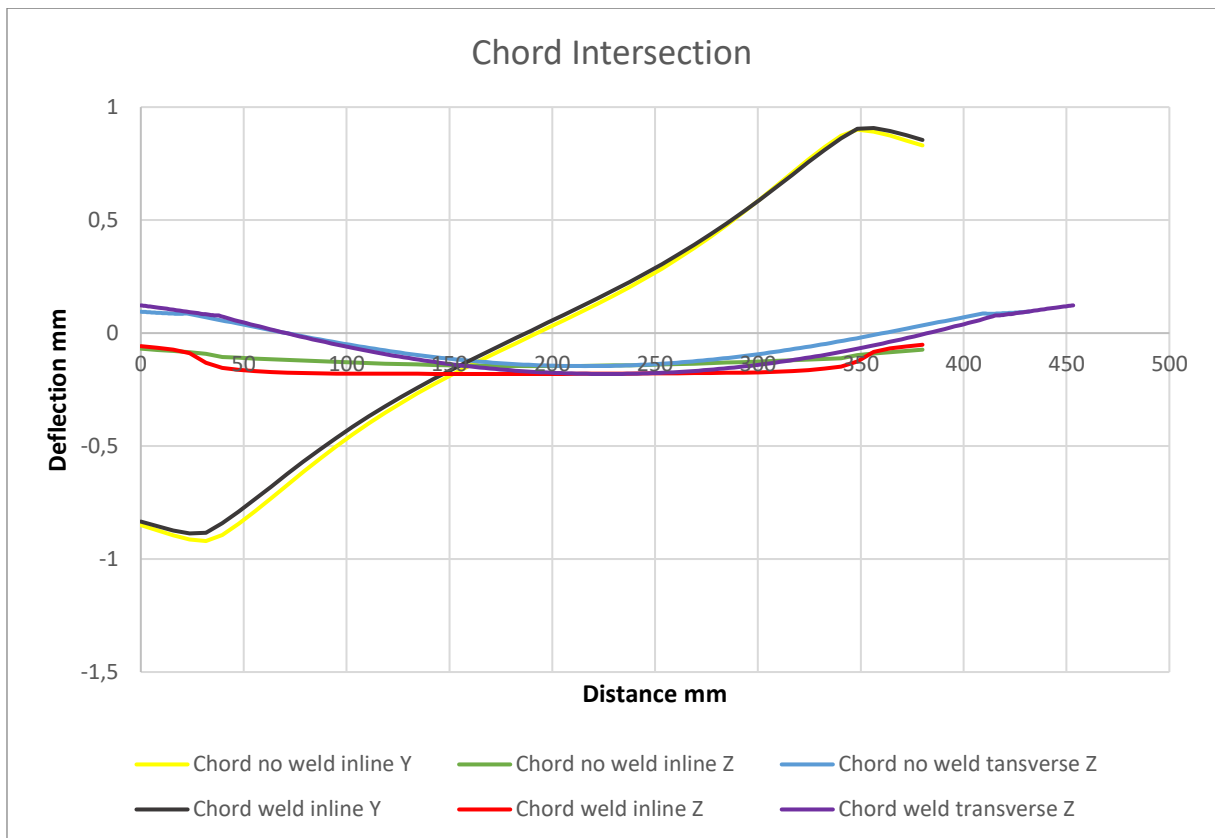
Figure 29 Deflection in line and transverse on the chord brace intersection
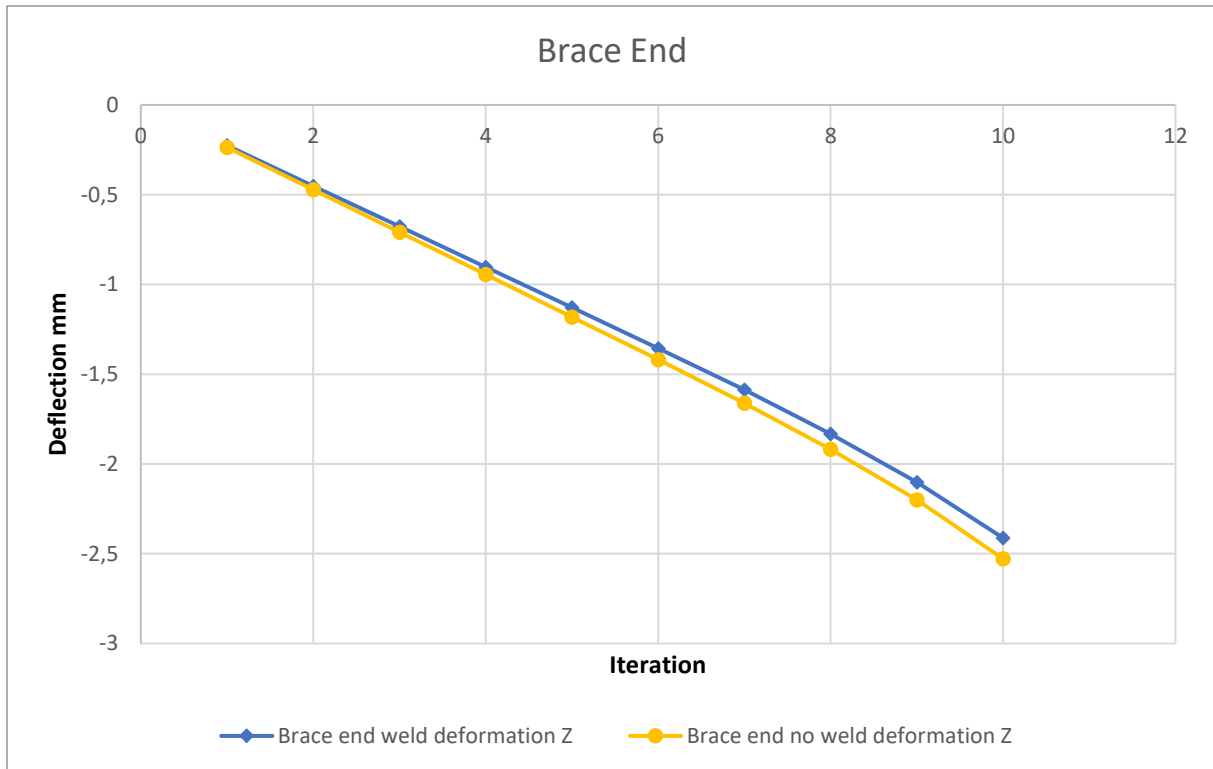
Figure 30 Brace end deflection

From the results in figures (27,28,29,30) there are no need to account for the weld, there are some differences when it comes to stress but deflection gives similar results. From the Figure 30 there can be seen that the brace end deflections are almost the same, and this is what affects the flexibility the most. By good confidence the weld can be omitted in the linear parametric study.

Since there was so much strain in the MSL test models (DT-, T-joint) from the MSL2000 report [3] the conclusion was made that strain could not be used for comparison. But the test models in the MSL2000 report [3] showed to capture the ultimate load capacity accurate with finite element and MSL nonlinear equation. TM-39 models were taken to the ultimate load capacity, and the strain here was large for the model without weld and reasonable for the model with weld. But for both the TM-39 models the ultimate load was far of in the finite element analysis. In ANSYS both models with weld and without weld gave an ultimate load to be about 3,4e8 Nmm which is far less than 4,3e8 Nmm from the MSL capacity. But since both models gave the same ultimate load, the weld can also be omitted in the nonlinear parametric study. The best way to determine deformation limits will be from experiments. Finite element can be used, but these results needs to be verified by real tests. In a tubular

50

joint there a multiple failure mode that needs to be accounted for, especially when defining a deformation limit.

The difference in time in figures (31, 32) is because how the time stepping was set. And some small differences were seen but the results are taken from where failure occurs in both models. Here the ultimate load was in the same range, so the results are comparable and do not give unnecessary error. From ANSYS a percentage difference was calculated, and it shows a 35% difference in strain between the models. But this number can change a lot depending on geometry, this can be seen in the MSL2000 rapport [3].
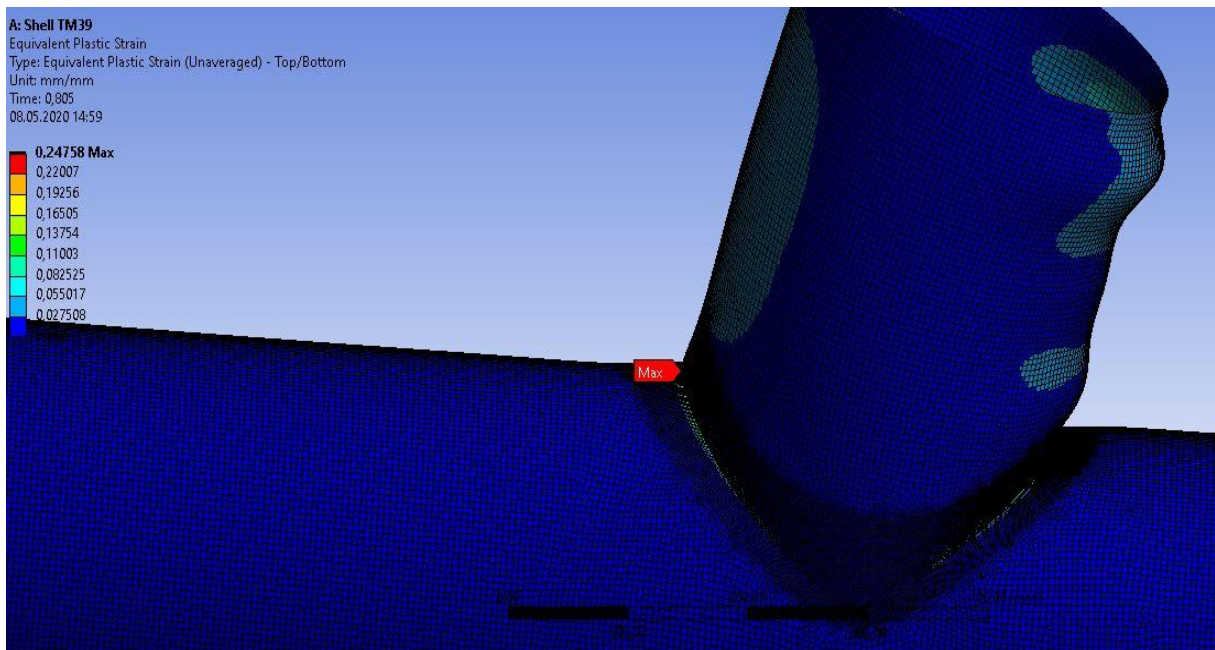
Figure 31 Ansys shell model without weld equivalent plastic strain
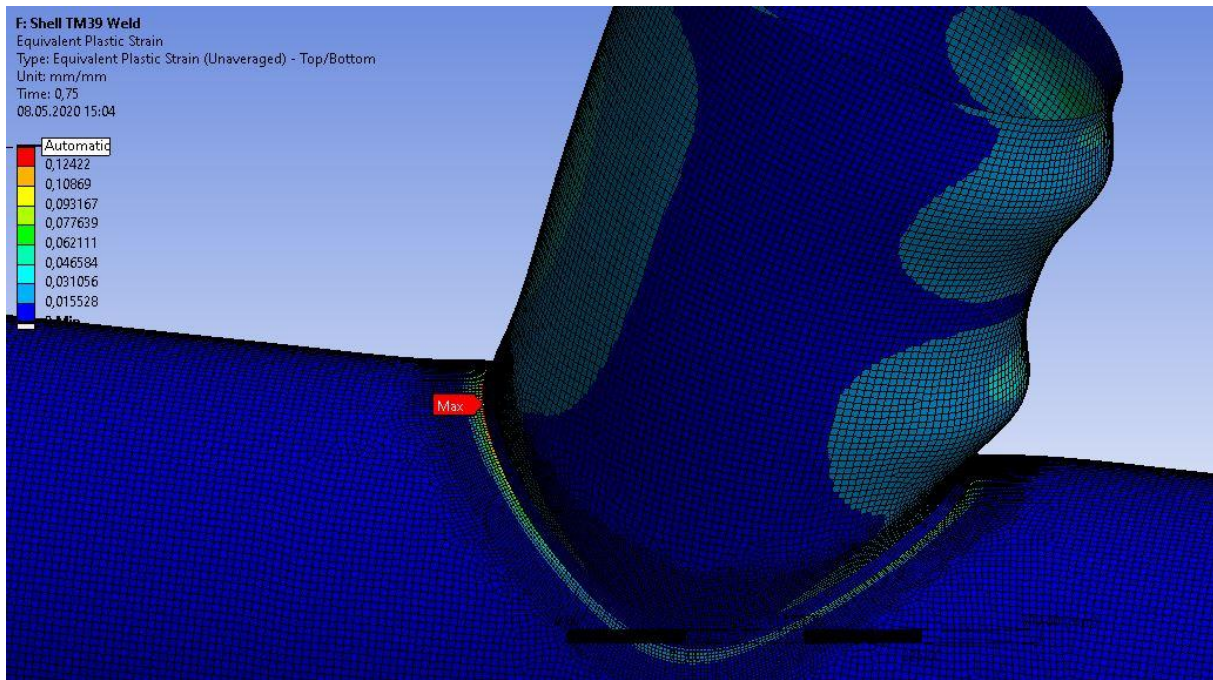
Figure 32 Ansys shell model with weld equivalent plastic strain

6 Parametric design study

6.1 Parametric setup

A parametric study will be done through the Ansys Designexplorer and the goal will be to create an automatic method that can calculate through many samples and output a dimensionless factor. This will be similar to what Buitrago did, but with a lot more samples and a more efficient way. And then naturally try to implement the eccentricity factor into Buitrago's out of plane bending equations. The input variables will then be beta, gamma, tau and eccentricity, angle of the brace has not been considered, all of these will be constrained to their respective validity ranges. Some extra constrains will be used on beta and eccentricity, because if beta becomes equal to 1 the stiffness will become Buitrago's out of plane bending scenario. The small restrictions on the validity range on beta and eccentricity will not affect the use of the equations. Because in the standards small deviations in eccentricity is allowed and the Buitrago equations covers that region. All the validity ranges are presented in Table 6.

Table 6 Validity range in parametric study

Validity Range		
	From	To
Beta	0,3	0,95
Gamma	10	30
Tau	0,25	1
Eccentricity	0,1	0,95

Since shell modelling without the weld are the chosen approach, all the equations created in Inventor to control the parameters must be done in such that they represent the same properties as the standards. The diameter cannot be the midsurface diameter, then small errors will already appear in the study. To control the Inventor model by the given variables, the outer diameter of the chord was set to constant and all the equations were driven from the outer diameter and the variables.

$$CHORD\_DIA\_OUT = 340,3$$

$$
\begin{aligned}
DS&\_OUT\_OF\_PLANE\_CHORD\_BRACE\_GAP \\
&= DS\_OUT\_OF\_PLANE\_ECC\_COEFFICIENT * ((((CHORD\_DIA\_OUT \\
&- CHORD\_THICKNESS)/2\,ul)) - (BRACE\_DIA\_OUT/2\,ul))
\end{aligned}
$$

$$BRACE\_DIA\_OUT = CHORD\_DIA\_OUT * DS\_Beta$$

$$CHORD\_THICKNESS = CHORD\_DIA\_OUT/(2\,ul * DS\_Gamma)$$

$$BRACE\_THICKNESS = CHORD\_THICKNESS * DS\_Tau$$

$$USC_i = (^{+}_{-}BRACE\_DIA\_OUT/2\,ul)^{+}_{-}80$$

Equation 39 Equations used in Inventor to control parametric model

The above equations control the parametric dimensions in Inventor and represents the equations used in the standards. The chord length must be constant, or it needs to be a variable because of the calculation of the chord beam rotation. The coordinate systems are also created in Inventor by equations. Then they will be at the same relative location in relation to the brace. The coordinate systems are used to split the surface to get the mesh algorithm to work equal each time. Triangular elements must be avoided in the region where the deflections are extracted. Because these elements are intended as filler elements [11].

To handle this a surface model based on the outer tubular dimensions were used, and then a function called thicken was used. And attached to Ansys Designmodeler through a solid part. All the splitting of surfaces, creating of surfaces and deleting of excessive surfaces are done in Designmodeler. The models will have problem with topology if this is done in Inventor. This means that as an example the chord and brace can be mistaken for two parts and not as one. For the analysis the best practice will be to implement them as one and get a uniform mesh from chord to brace. This will prevent the work of mesh realignment and pinching of chord-brace intersection.
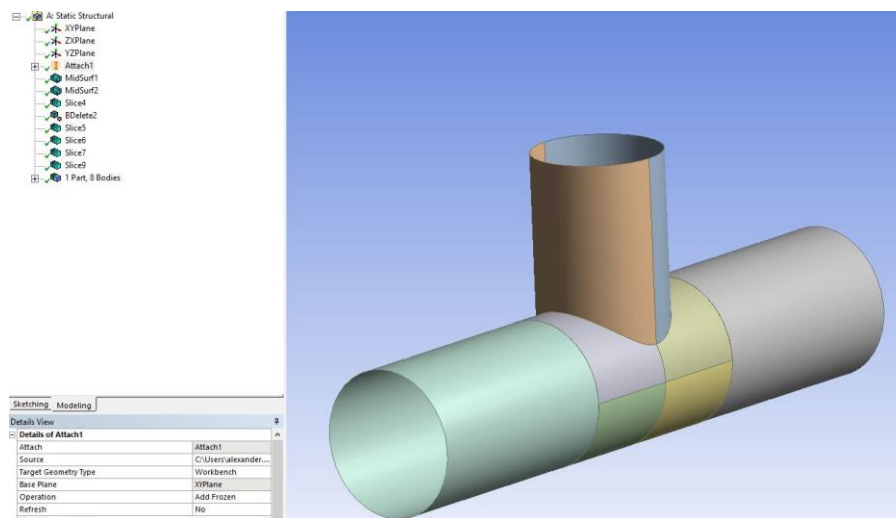
Figure 33 Cad model prepared for mechanical in designmodeler

From Designmodeler the model was transferred to Mechanical where pre-postprocessing was done. Named selection were created to handle the extraction points for the deflections used to calculate the chord-brace intersection rotation. Named selection is a good tool for ensuring that the model update do not lose the objectives created in Mechanical.

Meshing can be a time-consuming activity and therefore larger elements are preferable when outside the area of interest. That is good practice, but this has not been done in this thesis due to the reason of minimizing faults in the mesh combined with reliability and consistency, therefore the mesh size was locked to 5 mm. But when the brace gets small in relation to the mesh size, a finer mesh would often be necessary, but since the elements uses quadratic formulation the mesh will not need to be as fine to capture the deflection. The important results are pure displacement and not high stress regions with steep gradients.
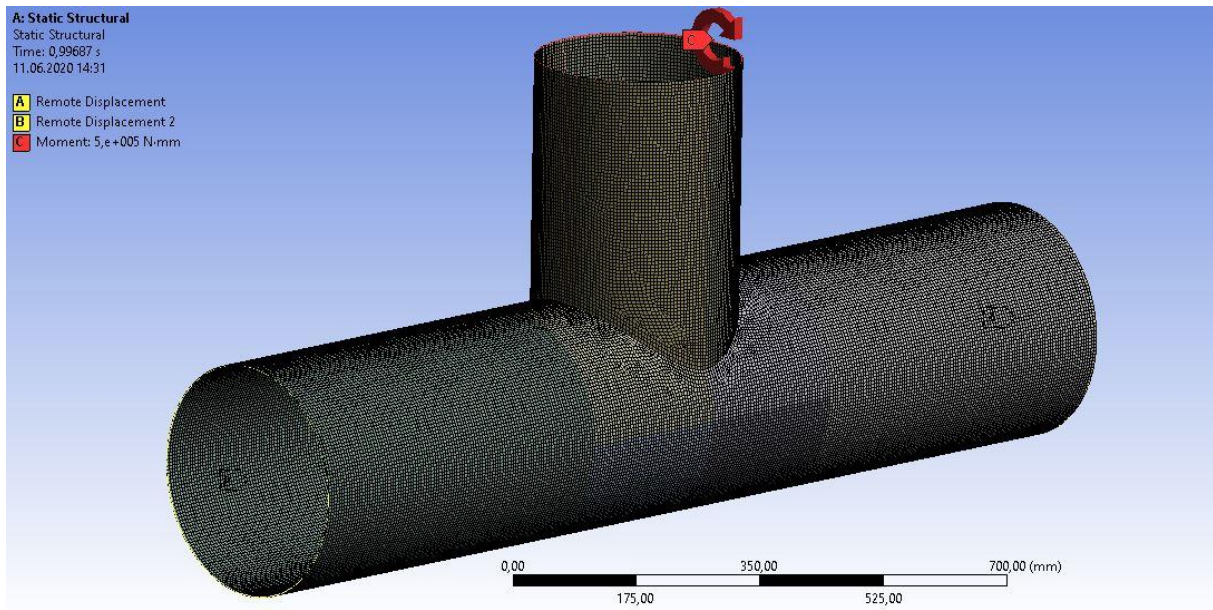
Figure 34 Meshed shell model in parametric study

From Figure 34 it can look excessive with the amount of elements but the solution time is 24 seconds for the solver. But that depends on the type of computer. The analysis is driven on 16 core processor and in core memory. The limiting factor for the speed of each iteration in the parametric study is the geometric updates. For reasons mentioned it is not beneficial to split and seed the shell model to reduce elements.

6.2 Ansys linear study

Buitrago's [9] equations and analysis are based on linear static analysis and this will also be done here. To generate the dimensionless factor f_{opb} for eccentricity the chord beam rotation must be calculated also at each iteration. This was done by using an analytic torsion formula in the parameter module in Ansys. Since calculation can be done by the Ansys at each geometric update inside the parametric module.

$$\alpha_{beam} = \frac{LT}{JG} \quad \begin{array}{l} L = Chord\ length/2 \\ T = Reaction\ moment\ chord \\ J = Polar\ moment\ of\ inertia \\ G = Shear\ module \end{array}$$

Equation 40 Angle of twist for linear torsion [18]

From NS_U1 and NS_U2 in Figure 35, which corresponds to global y displacement in the model, the net rotation in the joint are calculated by taking the algebraic difference between

55

these values and divide it by the brace's midsurface diameter. The dimensionless formula based on the net rotation is shown by the formula below, and it comes from Buitrago [9].

$$f_{opb} = \frac{\left(\left(\frac{(NS\_U1 - NS\_U2)}{D_{midsurface}}\right) - \alpha_{beam}\right)ED^3}{M}$$

Equation 41 Dimensionless formula from Buitrago [9]
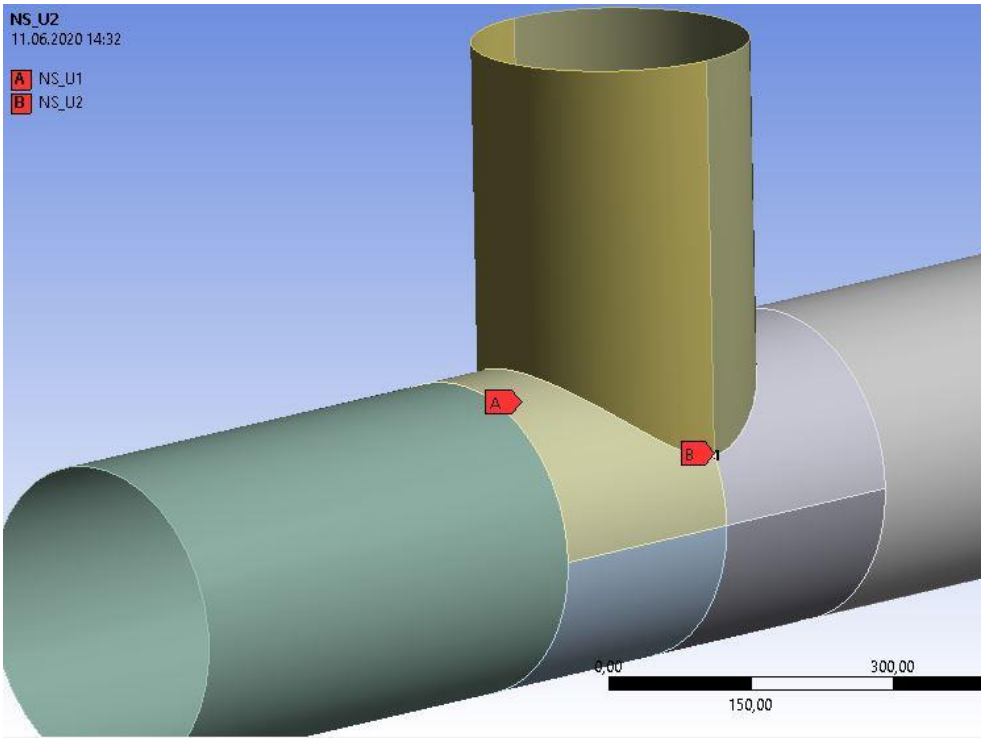
Figure 35 Global Y displacement for calculation of net rotation

The linear static analysis also makes it possible to make the moment load constant, since solving of the linear relationship between stiffness and displacement. Another benefit here is that Ansys will solve that equation in one iteration with the direct sparse solver. But in order to control that Ansys changes the model according to the parameters, output variables from each iteration can be used to track the model. Output variables can come from Mechanical and Inventor. This is very beneficial for values needed for further calculation or controlling mesh through the mesh metrics outputs.

When all the equations and output are set up in the parametric study, the design of experiments (DOE) can be generated. Here optimal space-filling (OSF) was chosen due to that Box-Behnken or central composites design will not work well for the setup here. Box-

Behnken in Ansys are a three-level quadratic design and locates at midpoints of the edges of the other variables. This will give few samples and would not give enough samples to really verify that all the combinations are covered. And the CCD a five -level factorial design but have a centre point and set the other design points from that. And can describe extreme points better than Box Behnken [11].
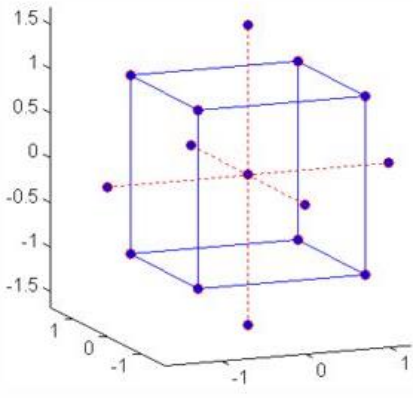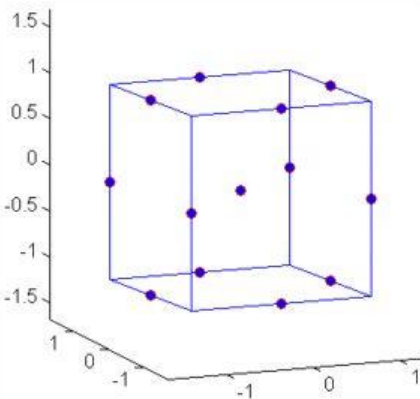
Figure 37 CCD [11]   *Figure 37 Box-Behnken [11]*

The optimal space filling (OSF) is a latin hypercube design (LHS) which is optimized and will prohibit design points to be close to each other. OSF will maximize the distance by the sampling points and optimize it to be uniform throughout the design space. This makes it an optimized LHS, which is an advanced Monte Carlo sampling method [11].
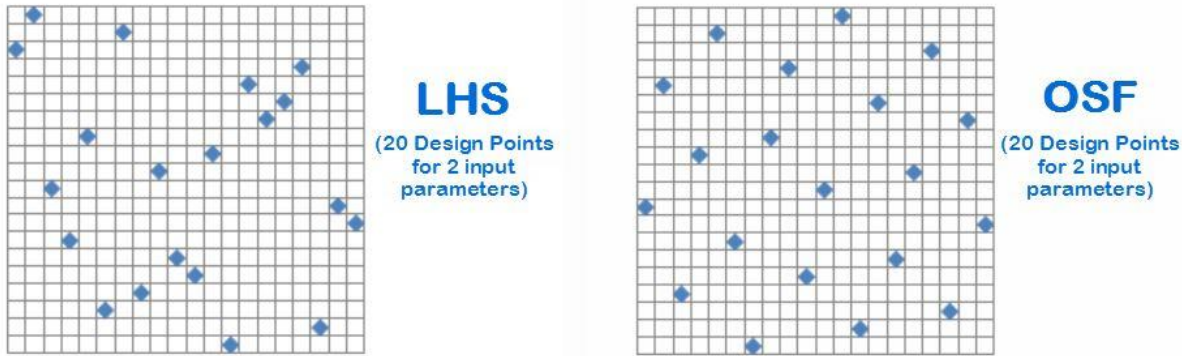
Figure 38 Latin hypercube and optimal space filling [11]

To improve the distribution of designpoints maximum entrophy was used. That will maximize the determinant of the covariance matrix which will give larger dispersion of the designpoints in the designspace. By the designspace the meaning will be inside the range of each variable.

The number of sampling points were set to 200, this comes from looking at the variables how they were distributed in the design space. But also, the goodness of fit, and if the verification points would have large error in relation to the predicted response. The tolerance was set to 10% on the predicted to the actual values and by 200 sampling points this was achieved.

In generating the response surface genetic aggregation with 30 verification points were chosen. This will give many points to check the predicted response against. The algorithm in Ansys uses a kriging with a gaussian kernel function and gives very good prediction. This can off course variate after the type of problem, the genetic algorithm finds the best suited approach. The type used on different output variables can be checked in the response surface log file. Then the goodness of fit can be checked and the local sensitivity of each input variable. This gives a lot of valuable information, that can be used for determining influence of variable and design points distribution.

To get an idea how each variable change with respect to the nondimensional factor, plots of each input variable can be plotted. This will be valuable to determine how the functions behave. Because the function and initial predictor coefficients needs to be guessed when doing the regression analysis. Even if the goal is to implement it into Buitrago's existing equation, the behaviour of the eccentric variable is unknown and the relation it has to the other variables. To determine what to do with Buitrago's equation each curve from Ansys were taken and a curve fitting exercise was done. By looking at what variables contributes to the change in stiffness of the tubular joint, it can clearly be seen that beta and gamma are the main variables.
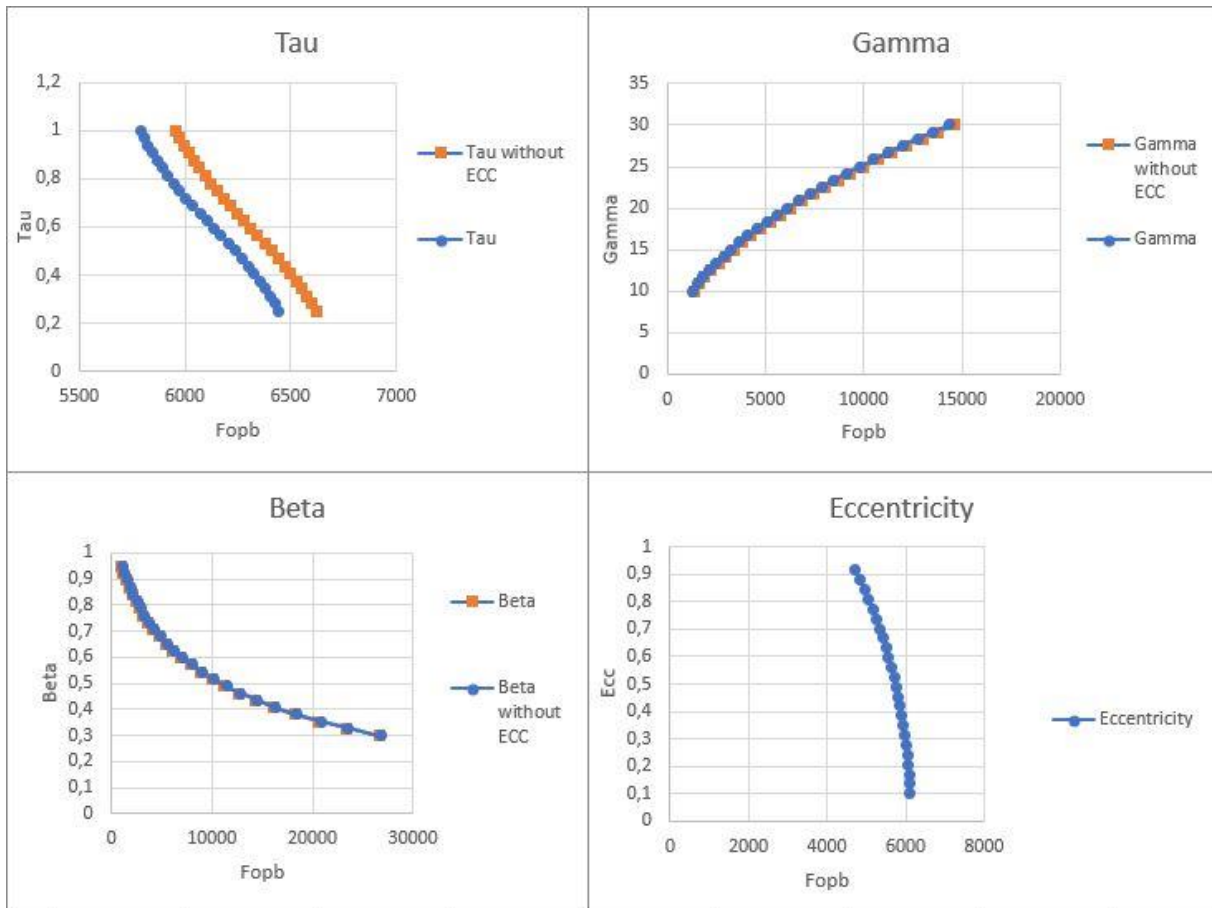
Figure 39 Beta,Gamma,Tau and Eccentricity as function of fopb

To be able to understand how much influence the eccentricity has on the t-joint, a parametric study without this factor was also done. And the influence when comparing equal designpoints only showed a reduction in tau. Beta and gamma were equal and that can indicate that the eccentricity does not have the big influence on the LJF as first believed.

$$y \sim (b1 * \exp(b4 * x2) * (-x3\text{\textasciicircum}b5) * (b2 * x1\text{\textasciicircum}b7 + b6) * (x4\text{\textasciicircum}b3))$$

Equation 42 Expression used to fit Ansys response

Equation 43 is the expression used in matlab for optimization and regression. Variables in the expression are x1(Eccentricity), x2(Beta), x3(Gamma) and x4(Tau). Matlab needs all the data as vector columns and to be able to do that the response and input variable are sent to excel as a csv file, and then cleaned up before they are transferred to Matlab. In Matlab the fitnlm command was used to fit the data to the function, which uses a nonlinear least square algorithm with the Levenberg-Marquette method implemented. From this the algorithm in Matlab hypothesis testing, residuals, R^2 and the coefficients standard deviation of the fitted function can be analysed. The p-value represents the hypothesis testing which can give information about the predictors [21]. Do they play a role in the model or are they

59

unnecessary for the model function response prediction? They should be close to zero or else they are not statistically significant in the model.

When using the Matlab command fitnlm [21] a warning concerning ill-condition of the Jacobian matrix comes, but the algorithm used for the nonlinear least square problem is the Levenberg Marquette which can handle these problems [15]. Ill-conditioning can result in that small changes in parameters gives large changes in response. The ill-condition can come from dependency in the variables or large variance in prediction variables. But more reason can also cause this low condition number. And when creating models simplified with less predictor variables that do not have problems with ill-conditioning, a new problem arises with the residuals in the fitting model. The fit becomes very poor but another phenomenon that should be careful with is overfitting the function.
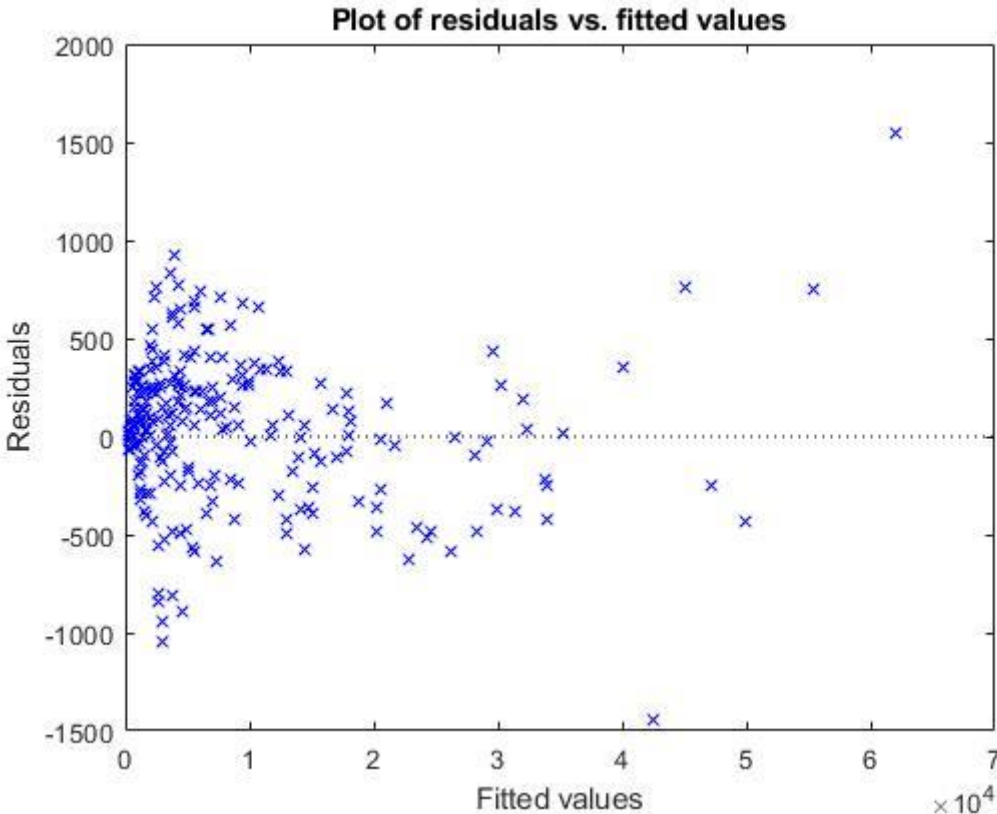
Figure 40 Residual plot for regression function

When looking at the residuals for the function fitted, there can be seen some symmetry. This should be random and evenly distributed and are not bad for the function. But the are some large residuals for the stiffer joints, which can show up to 30% deviation in fitted values to

60

actual values. Buitrago's equation has up to 25% deviation in his values [9] but he based his fitting on about 30 models which means that higher deviations can exist. Since less of the range is covered by data. R squared for the function Buitrago created was 0.98 and the function in this thesis with the added eccentricity is 0.99. The prediction slice in Figure 41 used in Matlab can also be used to see how the different variables functions changes throughout the range and compare them against Ansys's curves.
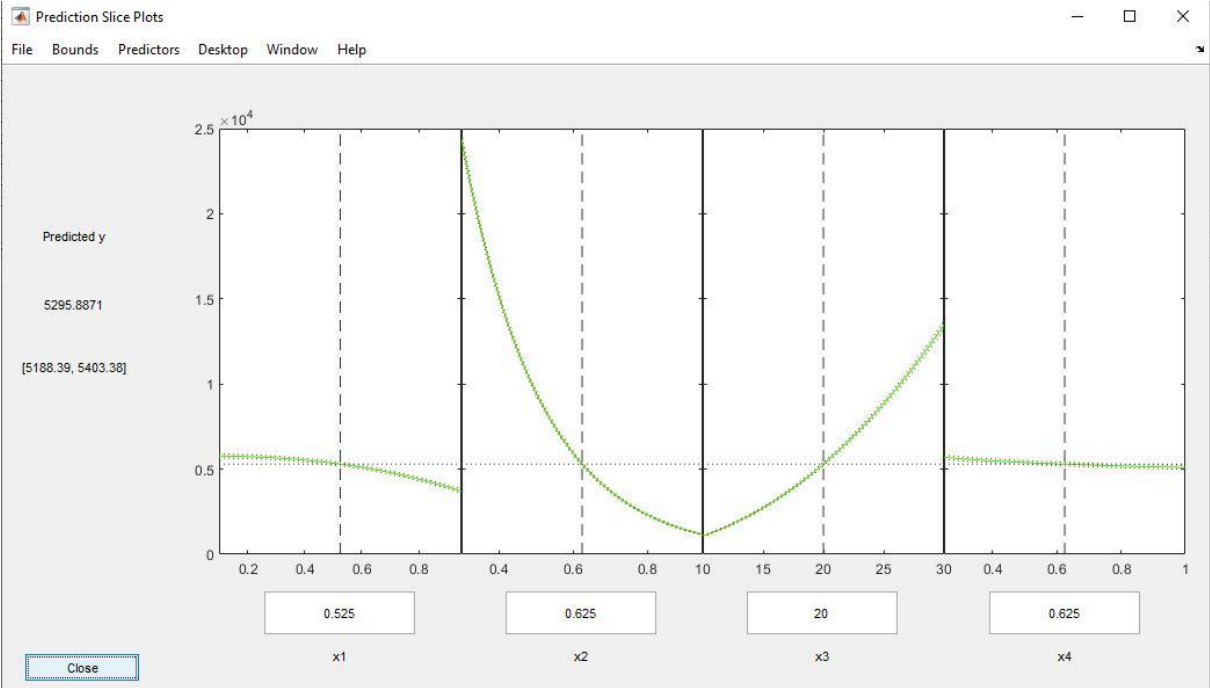
Figure 41 Prediction of variables in Matlab

As an attempt to test if the optimize algorithm in Matlab can refine the results generated by Levenberg-Marquette nonlinear least squares algorithm. The regression was done by interior-point algorithm through the minimizing of the objective function shown below. For a more detailed explanation of the interior-point algorithm go to [21].

$$\frac{objective}{minimize} = sum\left(\frac{y_p(b) - f}{f - \frac{f}{n}}\right)^2$$

Equation 43 R squared [21]

61

Goodness of fit plot was created to see how it performed. To use the optimization algorithm to do regression works well but gives more work when it comes to post processing. More coding must be done to get the output wanted to verify how the optimization algorithm performed.
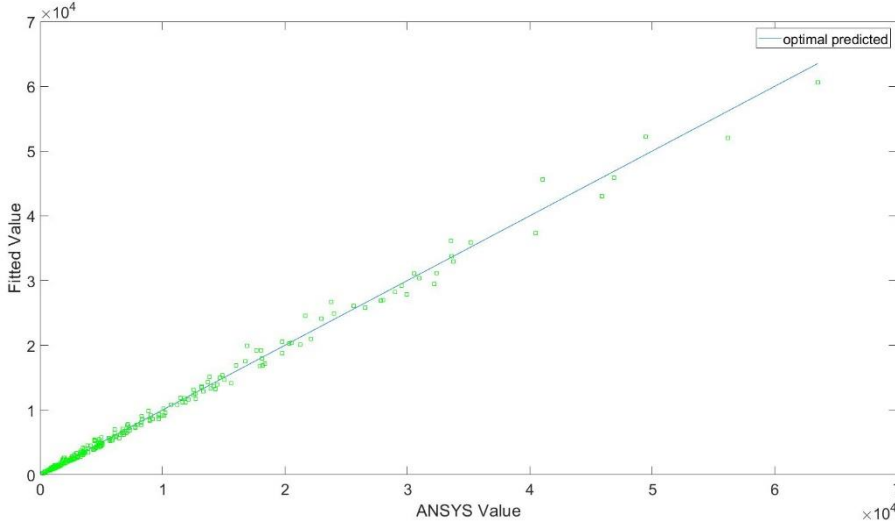
Figure 42 Goodness of fit plot optimization

Polynomial regression was also tested by implementing a polynomial expression. To capture the response closely beta became fifth order, the other variables were second and first order terms. This expression became too large to be handled as a formula for hand calculations but can easily be implemented by a computer. Again, if one tries to search for responses from outside the fitted data will the function be able to predict this.
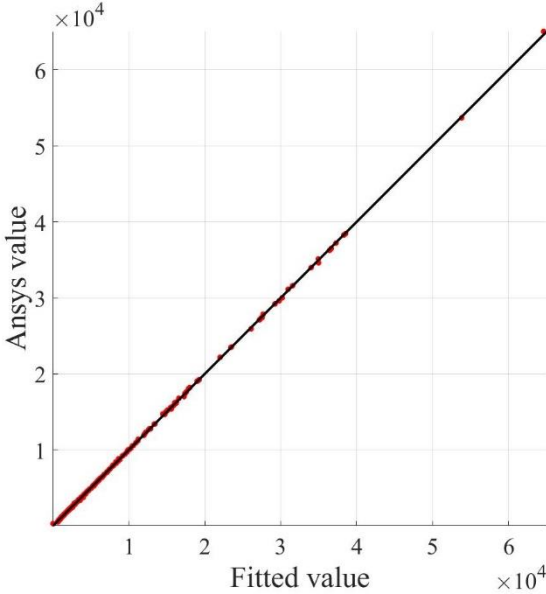
Figure 43 Goodness of fit polynomial regression

62

After the exercises above the final equation came together as input from all the curvefitting and regression work. It has the basis from Buitrago but the high "jumps" in values Buitrago's orginal out of plane bending has been "tuned"down. It is notable when comparing all the model's, that eccentricity do not have a huge impact on the structural response. This does not mean that it is applicable to other joints as K-, X or with T/Y-joints with angle implemented.

$$f_{opb_{ecc}} = \left(13.767e^{(-4.696beta)}\right) * \left(-gamma^{2.303}\right) * \left(3.1349Ecc_{coeff}^{2.444} - 7.6888\right) * \left(tau^{-0.0803}\right)$$

Equation 44 Fopb equation with eccentricity
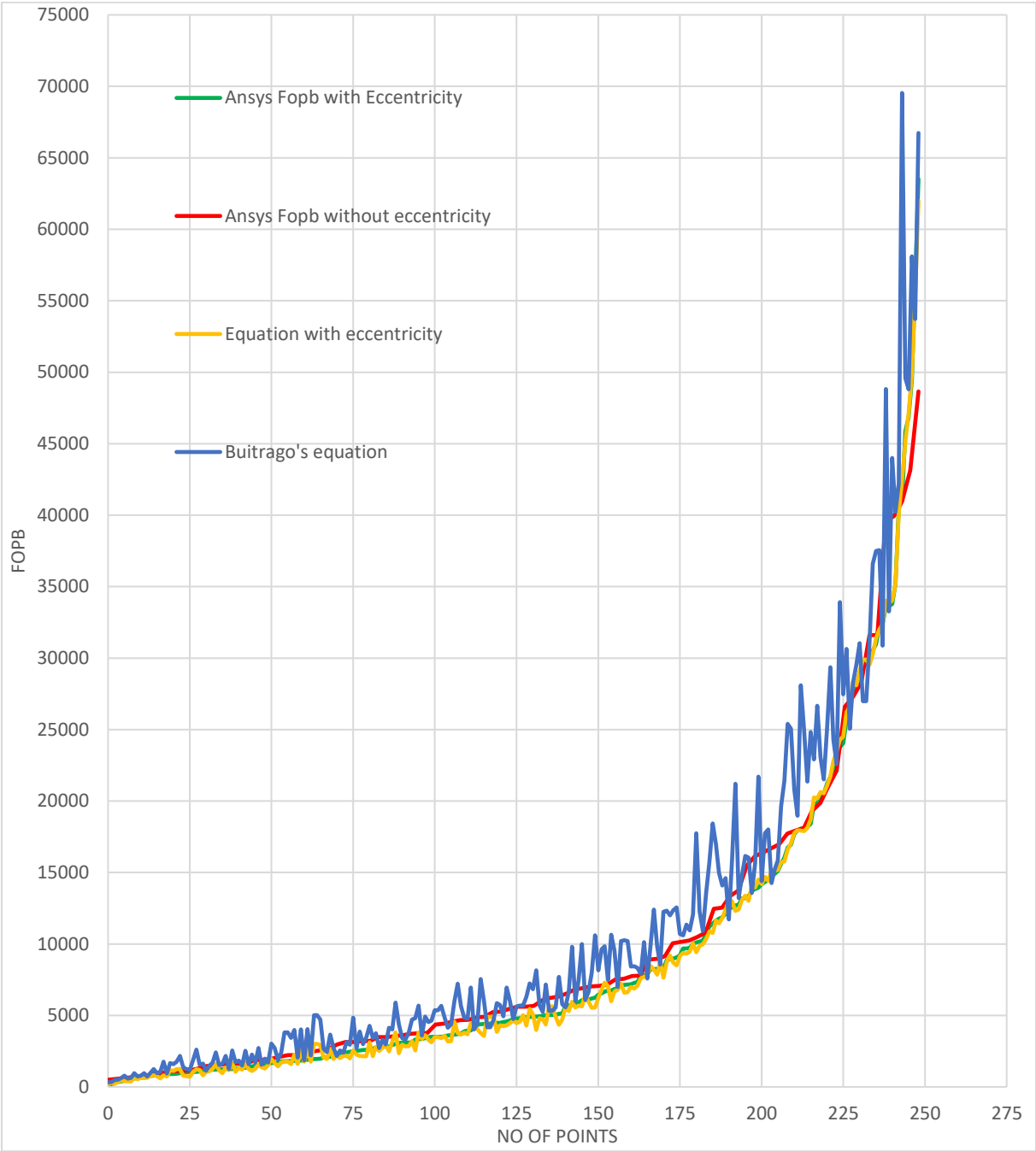
Figure 44 Comparison between different models

63

After implementing eccentricity into Buitrago's equation [9] the problem area is when beta is high, and gamma is low. This can perhaps be fixed through splitting the validity range up and generate separate equations for each range. But to use the data and functions generated from either optimization, polynomial or nonlinear regression, experimental data will be needed to do a validation study. The work that can be done by Ansys will indeed reduce the amount of experimental test needed. The most important will be to verify how the functions will behave outside the design points, and to verify that the errors generated then are within a reasonable range.

6.3   Ansys nonlinear study

The validation part against MSL nonlinear equation was done with large strain and geometric displacements. And the material curve was generated by Matlab from the DNV C208 standard [14]. MSL points out that the difference between bi linear and multilinear material data should not give large differences [3]. Here, as can be seen in Figure 11, the multilinear approach is used. From the linear study much of the approach towards the study into the nonlinear capacity is the same, but more challenges where met. Solving these numerical models takes a lot more time and more convergence issues arise. Direct solver with auto timestep and Newton-Raphson with line search were used. One issue with this is that that algorithm cannot handle when the force-displacement curve turn. This ensures that the loads are never larger than at the top of the curve. But again, the fracture aspect of the joints is not being considered and this becomes important for joints experience unloading and loading scenarios. The other algorithm which could be used is the arc-length method, and this can handle the negative force-displacement curve. This can be done through APDL commands into mechanical or switch to mechanical APDL and do the analysis and postprocessing there. But the arc-length method does need improvement to be efficient in Ansys, because a lot of trial and error with the maximum and minimum arc radius and step size must be done to get convergence. Using Newton-Raphson in these analyses will save time, but both methods need the analyst to check each analysis to verify if the ultimate load has been reached with the Newton-Raphson or gone past the top point with the arc-length method.

Drawback with nonlinear analysis is how sensitive it is. Mesh, stepping of the load, nonlinear stabilization and partition of model can influence convergence and results. As mentioned for the MSL2000 [3] T-joint in chapter 5.3 about validation. This makes more challenges when it comes to parametric study. Because the geometry keeps changing all the time and all the work by refining each model to perform is not possible in the same degree as when working with

one single model. These reasons will create uncertainties when it comes to the load-displacement in each joint, to calibrate this experimental work needs to be compared against the FEA.

To be able to set up the parametric study of the nonlinear T-joints almost a guess needs to be done on the moment loading. First eigenvalue buckling was used to achieve a pattern which could be used to optimize the ultimate load, but since these joints are stiff the eigenvalue buckling estimates to high and not in a uniform manner. The approach was to use the first joints calculated and do a qualified guess based on these. On the first joint a very high load was used and then it was adjusted to the last converged timestep (substep). In generating the design of experiments Box-Behnken was used together with manually filling out the missing points. These points are the outer or "extreme" points in the validity range. This resulted in a doe of 28 design points. Doe is made with min, mean and max for each input variable, to get more points would be beneficial but to calculate the 28 points are time-consuming. Tau was excluded from the analysis as an input variable, because the linear part showed to be mostly influenced by beta and gamma. Tau has been locked to 0.6, to add tau can improve the equations created but can also be satisfactory without. MSL has also excluded tau from the basic resistance, so only one more variable will be added and that is the eccentricity variable.

Basic resistance is presented in Equation 5 and the Q_u factor is where the eccentricity will be implemented. And a comparison between Ansys, MSL and the new equation with eccentricity was done. Here the basic resistance formula from MSL is performed reasonable according to Ansys. And since there are made a characteristic formula to be sure overestimating of the ultimate load does not occur. As in the linear the eccentricity plays a role but not increasing or decreasing the ultimate load by large amounts. But each variable has a contribution and design points where tau is changed to observe the change would be beneficial. The new equation with eccentricity implemented is presented below.

$$M_{Ecc\ opb} = F_y T^2 d^{2.133}(0.074\gamma^{(0.0687\beta^{-1.099})}0.182Ecc^{0.103})$$

Equation 45 Basic nonlinear capacity equation with eccentricity

The minimizing of the objective which is R squared is at about 98.5 percentage, but there can be seen from the residuals and the comparison between Ansys and the equation that there are clearly areas that need improvement to get a more accurate equation.
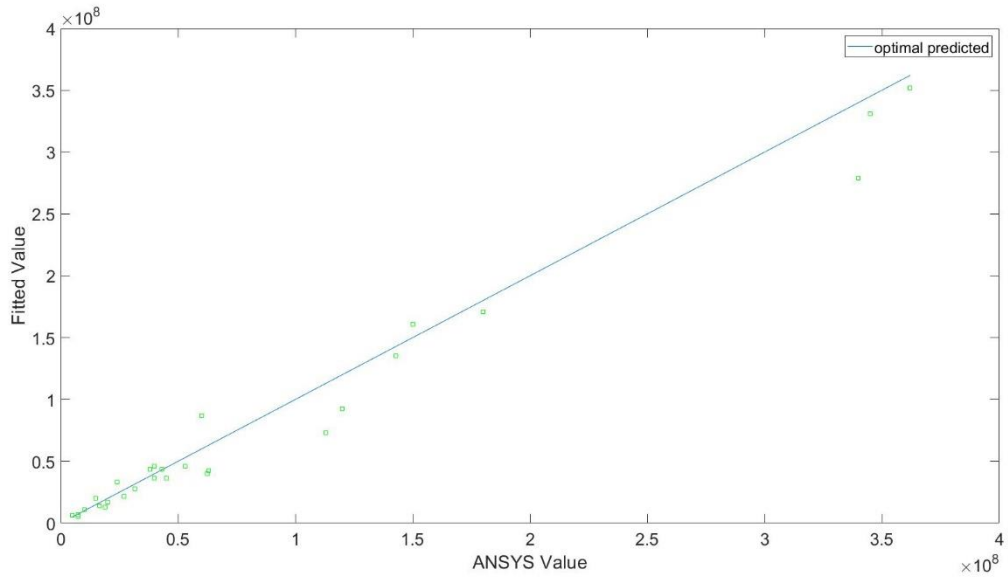
Figure 45 Goodness of fit plot optimization of capacity equation
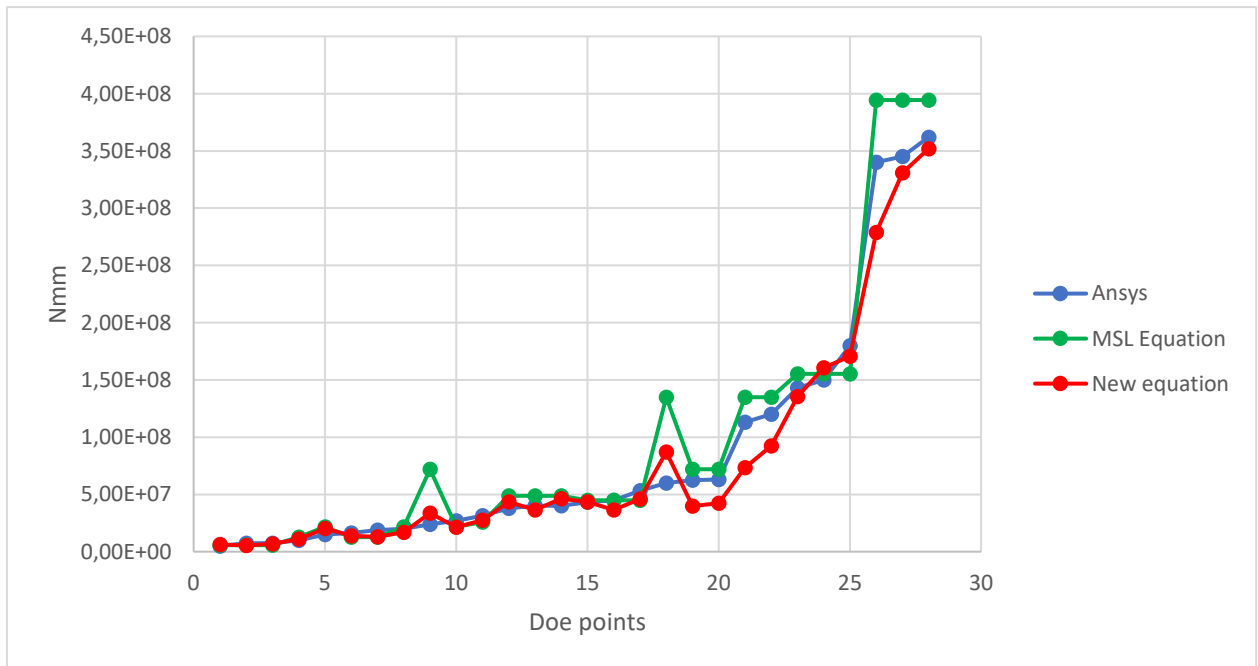
Figure 46 Comparison between different Ansys,MSL and new equation

7 Conclusion

At the outset of this study an assumption was that the out of plane eccentricity influences the response of the T-joint to some extent, but there can be seen that the influence is not that great. This can be seen from both comparison in the linear regime and on nonlinear capacity. Refinement of the earlier function by regression, function evaluation and design points can be just as important as to implement the eccentricity. And by this further work on improving equations that will cover certain validity ranges could be more beneficial. When the equations show a smaller difference to the real response, then include more variables like eccentricity. A clear conclusion can first be taken after all the data in this thesis is compared and calibrated against experimental data. But the shell model had good agreement against the validation cases performed. Because of this some confidence in the generated data and therefore the data can contribute to some conclusion about eccentricity and performance of the equation created in the thesis.

Equations created in the thesis shows to fit the response well for both linear with eccentricity and nonlinear capacity with eccentricity. In the linear case Buitrago's [9] out of plane bending equation without eccentricity has a fluctuating response in through the validity range, this has been improved in the equation with eccentricity. The R squared of the fitted model is 0.99, which is higher than Buitrago's [9] equation for out of plane bending without eccentricity, but the residuals deviation of up 30 percent between fitted value and Ansys response for the equation created here is higher than Buitrago's 25 percent. But this can be argued to come from the amount of design points analyzed in the thesis. The implementation of eccentricity in Buitrago's equation [9] does give an equation that performs reasonable. For the nonlinear capacity a R squared of about 98.5 percent was achieved and it follows the Ansys response good. And the MSL equation [3] without eccentricity follows the Ansys curve which gives some indication that the ultimate loads taken from Ansys are not too of. Because that the nonlinear models are much more sensitive to mesh and numerical errors, and this can give ultimate loads that can be far away from the turning point in the force displacement curve. For this reason, a safety margin needs to be implemented like the characteristic MSL load [3].

Parametric study done this way like in this thesis gives an efficient way to study large amount data for a structure. Especially for linear static analysis, the nonlinear static analysis gives more manual work, but it will reduce the amount of experimental work needed in both cases. And the to get an indication on how each variable change with respect to the other are achieved as output from the parametric study, which makes further predictions easier.

8 Literature

[1] R. Khan, "Structural Integrity Management and Improved Joint Flexibility Equations for Uni-Planar K-Type Tubular Joints of Fixed Offshore Structures", Ph.D. dissertation, Engineering, London South Bank University, London, 2016. Available: doi:10.18744/PUB.001470

[2] USFOS, Joint Capacity Theory Description of use Verification**,**.2019.

[3] MSL Engineering Ltd, "JIP – Assessment Criteria, Reliability and Reserve Strength of Tubular Joints (Phase II)", MSL, Berkshire, United Kingdom, Document No C20400R014 Rev 0, July 2000.

[4] MSL Engineering Ltd, "The effects of local joint flexibility on the reliability of fatigue life estimates and inspection planning", 2001/056, 2002

[5] Design of steel structures, N-004, 2.10.2016.

[6] *Recommended Practice for planning, Designing and Constructing Fixed Offshore Platforms- Working Stress Design,* RP 2A-WSD, 26.10.2007

[7] *Petroleum and natural gas industries- Fixed steel offshore structures,* ISO 19902, 2007.

[8] Ø. Hellan, "Nonlinear Pushover and Cyclic Analyses in Ultimate Limit State Design and Reassessment of Tubular Steel Offshore Structures", Division of Marine Structures, The Norwegian Insitute of Technology, Trondheim, 1995

[9] J. Buitrago, B.E. Healy and T.Y. Chang, "Local Joint Flexibility of Tubular Joints", OMAE – Volume 1, Offshore Mechanics and Arctic Engineering Conference, ASME, Glasgow, 1993.

[10] R.D. Cook, D.S. Malkus, M.E. Plesha and R.J. Witt, *Concepts and Applications of Finite Element Analysis,* 4th ed., USA, John Wiley & Sons, Inc, 2002. S.1-719

[11] ANSYS, Welcome to ANSYS Help, 2020. Available https://ansyshelp.ansys.com/account/secured?returnurl=/Views/Secured/main_page.html

[12] O.C. Zienkiewicz, R.L. Taylor and J.Z Zhu, *The Finite Element Method: Its Basis and Fundementals*, 6th ed., Amsterdam, Elsevier, 2005. Available: https://ebookcentral-proquest-com.ezproxy.uis.no/lib/uisbib/detail.action?docID=288930

[13] K.J. Bathe, *Finite Element Procedure*, 2th ed., Englewood Cliffs N.J, Prentice Hall, 1996.

[14] *Determination of structural capacity by non-linear finite element analysis methods*, DNVGL-RP-C208, 2016

[15] G.A.F Seber & C.J Wild *"Nonlinear regression"* Department of Mathematics and Statistics Unuversity of Aucland, Aucland New Zealand, 2003.

[16] *Fatigue design of offshore steel structures*, DNVGL-RP-C203, 2016.

[17] *Eurokode 3: Prosjektering av stålkonstruksjonet Del 1-5: Plater påkjent i plateplanet*, NS-EN 1993-1-5:2006+ NA:2009, Okt. 2006.

[18] Epsilon, "Stabilization Damping for Nonlinear Convergence" Nov. 2019, Available: https://www.epsilonfea.com/wp-content/uploads/2019/11/ANSYS-Nonlinear_Stabilization_User_Meeting_2019Nov20.pdf

[19] Engineering ToolBox, (2005). *Torsion of Shafts*, 23.04.2020. Available: https://www.engineeringtoolbox.com/torsion-shafts-d_947.html

[20] M, A, Atteya, "Personal communication", 24.02.2020.

[21] Matlab, Help documentation, 2020. Available: https://www.mathworks.com/help/

9 Appendix

9.1 Ansys output data for study with eccentricity

P32Beta	P33Gamma	P34Tau	P47ECC	P40Fopb
0,9486	10,2977	0,9786	0,8686	197,7019475
0,9432	10,2140	0,9236	0,1176	203,3180283
0,9139	10,0542	0,2572	0,9131	246,5910996
0,9159	11,3500	0,7431	0,4634	339,6553587
0,9126	11,6500	0,4319	0,2296	378,294894
0,9451	13,6500	0,4019	0,7779	422,3994741
0,8411	10,2500	0,5144	0,6419	440,7939909
0,8964	12,1500	0,7394	0,8034	458,7362389
0,9224	14,5500	0,5256	0,5186	592,7165463
0,8379	11,8500	0,9381	0,6334	618,9917662
0,8639	12,8500	0,9306	0,2934	655,1452615
0,8574	12,4500	0,3081	0,5654	655,6696951
0,7534	10,1500	0,7881	0,3401	693,7042251
0,8606	13,5500	0,6606	0,2211	774,6652972
0,9289	17,0500	0,7844	0,6121	784,1184955
0,7956	11,7500	0,5106	0,3699	816,3875619
0,7859	12,0500	0,5369	0,8969	838,4189344
0,9500	20,0000	0,6250	0,9500	859,8422081
0,7144	10,5500	0,7506	0,6801	875,4518955
0,9484	19,6500	0,7019	0,3189	904,8541751
0,9500	20,0000	1,0000	0,5250	910,9023771
0,9500	20,0000	0,6250	0,1000	929,2707838
0,9500	20,0000	0,2500	0,5250	950,0504198
0,8866	16,6500	0,9194	0,8374	974,2541143
0,6250	10,0000	0,6250	0,9500	1027,773637
0,7566	12,6500	0,8781	0,9054	1027,803537
0,9354	19,8500	0,5856	0,7524	1029,604702
0,9498	21,7826	0,2759	0,8126	1057,282939
0,9061	18,1500	0,8669	0,1574	1065,369202
0,8769	17,2500	0,6906	0,9436	1117,004489
0,6250	10,0000	1,0000	0,5250	1143,500888
0,7826	13,0500	0,2856	0,2509	1151,675766
0,8899	18,4500	0,9606	0,4804	1211,609463
0,9410	21,9501	0,5028	0,3438	1217,423228
0,6250	10,0000	0,2500	0,5250	1233,220363
0,7176	12,2500	0,3231	0,8161	1241,812096
0,8931	18,3500	0,2819	0,4081	1242,435278
0,6250	10,0000	0,6250	0,1000	1252,59779
0,9419	22,3500	0,4656	0,3869	1253,310714
0,8216	15,5500	0,4806	0,7439	1284,933889
0,8541	16,8500	0,4619	0,2976	1328,789268
0,6331	10,4500	0,3756	0,4761	1330,688194
0,9064	19,8980	0,2658	0,1080	1343,340818
0,7891	14,9500	0,8294	0,4846	1395,470337
0,8444	17,4500	0,3269	0,8841	1438,894297
0,5974	10,6500	0,5181	0,7396	1477,699878
0,9321	23,9500	0,8894	0,7651	1485,988077

0,7306	13,4500	0,8406		0,1149	1518,214197
0,7761	15,8500	0,7356		0,7736	1617,635898
0,6006	10,9500	0,6306		0,4549	1663,286609
0,9191	23,8500	0,6756		0,5526	1667,794472
0,8704	20,0500	0,3944		0,6249	1687,183485
0,7111	13,7500	0,5894		0,6079	1701,146024
0,8346	18,6500	0,6344		0,4974	1781,637334
0,9435	28,1655	0,9400		0,9475	1806,503408
0,9435	28,1655	0,9400		0,9475	1806,503677
0,9029	23,6500	0,4694		0,9096	1816,448233
0,9256	25,3500	0,3344		0,6036	1819,827745
0,5259	10,7500	0,9156		0,8204	1839,1242
0,9381	27,0098	0,5106		0,1334	1848,522265
0,5551	10,8500	0,8931		0,5059	1876,738313
0,9386	27,6500	0,6381		0,3614	1897,338072
0,7339	14,7500	0,4469		0,1234	1938,553229
0,9491	29,3768	0,3824		0,4490	1955,704277
0,9491	29,3768	0,3824		0,4490	1955,704283
0,9500	30,0000	0,6250		0,5250	1981,546363
0,8249	19,1500	0,6269		0,1064	2045,111815
0,7924	17,8500	0,7731		0,2594	2063,613501
0,9094	26,1500	0,9419		0,3019	2109,457539
0,7469	16,3500	0,4056		0,5229	2192,792096
0,5389	11,2500	0,9269		0,1999	2286,805423
0,6299	13,9500	0,8631		0,6886	2348,408874
0,6461	14,1500	0,9944		0,4166	2390,682365
0,7989	20,2500	0,8819		0,6546	2419,408695
0,5779	13,3500	0,7206		0,8756	2445,546918
0,8996	28,0500	0,6794		0,8331	2505,492261
0,6949	15,6500	0,6719		0,3741	2520,884273
0,8281	22,7500	0,7056		0,8459	2545,081507
0,6981	16,9500	0,9981		0,7566	2584,79966
0,5291	12,5500	0,4281		0,9181	2586,784566
0,8801	25,9500	0,7244		0,1446	2608,306529
0,6591	15,7500	0,5069		0,8289	2692,014658
0,8314	22,9500	0,8481		0,3996	2708,849848
0,6201	14,0500	0,8369		0,2891	2732,281879
0,7729	19,9500	0,9756		0,2424	2817,726214
0,4284	10,0500	0,4956		0,3486	2821,338591
0,7436	18,5500	0,2669		0,6929	2839,342765
0,8323	23,8630	0,9205		0,1105	2940,198981
0,8834	27,8500	0,3456		0,2466	3000,300145
0,7599	21,8500	0,9044		0,9479	3061,154581
0,5584	12,7500	0,3194		0,1786	3093,845504
0,6104	14,2500	0,4769		0,3231	3095,618529
0,6169	14,4500	0,2631		0,4676	3100,727255
0,8086	22,4500	0,3606		0,3826	3123,112719
0,7241	20,4500	0,5556		0,9266	3312,773933
0,8671	29,0500	0,8744		0,5739	3338,099341
0,4219	11,1500	0,7131		0,6291	3361,084864

0,8184	24,4500	0,6231		0,3104	3415,293256
0,4771	12,3500	0,2781		0,7354	3462,849192
0,7371	20,5500	0,5519		0,6631	3504,249737
0,3622	10,8454	0,2610		0,9168	3504,736769
0,3622	10,8454	0,2610		0,9168	3504,736769
0,8151	25,1500	0,4731		0,7014	3513,943955
0,8021	24,6500	0,9794		0,5399	3540,86248
0,6624	17,7500	0,7281		0,6164	3596,730867
0,5844	15,0500	0,3869		0,6674	3620,1492
0,8662	29,9941	0,9876		0,1433	3657,221164
0,8509	28,8500	0,3719		0,7821	3689,565599
0,8119	26,0500	0,7544		0,6844	3706,647678
0,3699	11,4500	0,6569		0,8629	3897,222772
0,6754	17,9500	0,3419		0,2679	3948,525012
0,8476	29,2500	0,5444		0,5611	3950,419441
0,3861	11,0500	0,7656		0,2721	4133,119122
0,6071	16,5500	0,6681		0,1659	4338,439569
0,7501	24,2500	0,2894		0,8714	4387,661979
0,6250	20,0000	1,0000		0,9500	4398,800198
0,3289	10,4499	0,9980		0,3013	4429,6992
0,3289	10,4499	0,9980		0,3013	4429,6992
0,3000	10,0000	0,6250		0,5250	4466,500629
0,6721	21,0500	0,8219		0,8119	4475,090077
0,3380	12,0239	0,9415		0,9458	4477,975564
0,6526	19,0500	0,8594		0,3784	4539,706165
0,7794	27,4500	0,9531		0,7949	4571,455252
0,7274	23,0500	0,7169		0,5441	4660,515689
0,4674	13,1500	0,5406		0,1404	4735,388972
0,4739	14,3500	0,5781		0,7311	4795,909576
0,6916	20,6500	0,5331		0,2339	4803,057709
0,3601	11,5500	0,4169		0,6504	4844,043806
0,4869	16,0500	0,9231		0,9224	4874,206204
0,8054	28,7500	0,8144		0,3146	4901,643273
0,7664	24,9500	0,4581		0,1319	4902,734928
0,6250	20,0000	0,2500		0,9500	4913,610094
0,7046	21,9500	0,8069		0,1531	4943,191439
0,5129	15,2500	0,7469		0,5314	4978,731472
0,6689	21,3500	0,4094		0,7906	5009,916279
0,3192	10,4233	0,3881		0,1099	5031,90291
0,3192	10,4233	0,3881		0,1099	5031,90291
0,4706	13,8500	0,4431		0,4889	5045,493525
0,5746	18,2500	0,3006		0,8926	5119,605073
0,5876	17,5500	0,5631		0,5271	5123,721027
0,4641	14,6500	0,9119		0,3911	5644,592929
0,6250	20,0000	0,6250		0,5250	5701,402555
0,7631	27,3500	0,2594		0,5781	5721,644223
0,6250	20,0000	1,0000		0,1000	5792,536696
0,6851	22,8500	0,5219		0,4421	5914,651455
0,7460	29,5000	0,7521		0,8674	6060,181573
0,3211	11,9500	0,9081		0,5484	6075,548651

0,4251	14,8500	0,9869		0,6971	6105,391995
0,5616	19,3500	0,6119		0,7991	6187,214234
0,7209	27,9500	0,5031		0,9011	6234,325027
0,6250	20,0000	0,2500		0,1000	6448,572522
0,7404	27,2500	0,4131		0,3954	6544,209658
0,7696	29,7500	0,5706		0,2169	6660,277296
0,3731	12,9500	0,3306		0,3529	6737,399961
0,6786	27,1500	0,7919		0,9139	6739,883986
0,6494	22,2500	0,2519		0,4506	6855,215291
0,4544	15,3500	0,6456		0,3274	6912,919095
0,7079	25,4500	0,2744		0,2126	7024,205268
0,4316	17,1500	0,5819		0,9394	7131,808771
0,6559	25,0500	0,6006		0,7694	7161,911411
0,3894	15,1500	0,8031		0,7864	7171,10519
0,5096	18,7500	0,8856		0,7099	7268,016674
0,6039	22,0500	0,9831		0,5144	7339,67243
0,5519	19,7500	0,9719		0,1914	7791,297979
0,6656	26,2500	0,8706		0,5994	7808,458674
0,4446	15,9500	0,8181		0,1191	7863,607342
0,6819	26,9500	0,9344		0,1829	8247,85296
0,7014	29,8500	0,7319		0,7184	8256,274954
0,5324	19,2500	0,3906		0,5016	8258,52498
0,3244	13,2500	0,5669		0,4464	8317,397782
0,5064	21,4500	0,7619		0,9351	8342,306787
0,3471	15,4500	0,3831		0,8671	8864,651394
0,6884	28,5500	0,6644		0,4336	8948,148602
0,6266	24,7500	0,3794		0,5824	8984,590296
0,5681	24,5500	0,9569		0,8501	9064,437398
0,6234	24,8500	0,8106		0,3316	9207,450199
0,5454	21,2500	0,6419		0,3359	9684,035262
0,5714	21,6500	0,3569		0,1021	9692,981354
0,5356	21,5500	0,7769		0,5101	9726,276796
0,6429	26,4500	0,6494		0,1701	10012,48419
0,6250	30,0000	0,6250		0,9500	10103,22991
0,5909	23,3500	0,3981		0,2764	10155,72266
0,4609	18,0500	0,4506		0,2636	10237,76547
0,4349	18,8500	0,4356		0,7226	10723,17248
0,5194	22,1500	0,2706		0,6716	11216,5611
0,4999	24,1500	0,4919		0,9309	11435,73107
0,6364	29,3500	0,4881		0,6461	11635,58537
0,5161	23,7500	0,7806		0,7269	11780,75228
0,4576	18,9500	0,2556		0,2849	11875,36681
0,6136	28,2500	0,9681		0,4209	12100,5425
0,3374	16,1500	0,9456		0,2381	12545,03335
0,6250	30,0000	1,0000		0,5250	12546,2044
0,5811	28,1500	0,3119		0,8246	12689,61043
0,4804	20,7500	0,6081		0,1106	12748,56634
0,4089	19,5500	0,7094		0,6206	13188,64163
0,3634	17,3500	0,2969		0,5951	13204,34346
0,4901	22,6500	0,5481		0,5909	13347,16998

0,3341	16,7500	0,7694		0,4251	13702,93973
0,3016	16,4500	0,6044		0,7056	13843,41514
0,6250	30,0000	0,2500		0,5250	13927,94071
0,4479	20,9500	0,8331		0,2806	14183,28536
0,6250	30,0000	0,6250		0,1000	14330,63752
0,5486	26,7500	0,6831		0,5696	14455,31482
0,3179	16,2500	0,5931		0,2084	14702,76537
0,3829	19,4500	0,9644		0,4931	14888,76622
0,3666	17,6500	0,3681		0,1276	15100,25676
0,5941	28,6500	0,4206		0,1616	15592,07575
0,4121	22,5500	0,5969		0,8076	16035,39083
0,5031	28,4500	0,6531		0,8544	16751,75902
0,3000	20,0000	0,6250		0,9500	16934,65228
0,3504	20,8500	0,9006		0,7609	17681,87458
0,4934	25,2500	0,7956		0,1361	17947,90539
0,4056	23,5500	0,3156		0,8586	18062,24918
0,4836	26,3500	0,4394		0,7141	18116,23198
0,5226	26,8500	0,5294		0,3444	18193,81367
0,5649	29,4500	0,3381		0,4124	18388,62642
0,5421	29,6500	0,7994		0,3061	19767,6252
0,4966	29,5500	0,8969		0,7481	19804,69796
0,4511	25,6500	0,8556		0,5356	20352,25381
0,3536	20,3500	0,5594		0,4379	20523,58971
0,4381	24,0500	0,3644		0,4294	21227,23006
0,3049	21,7500	0,6981		0,8884	21680,14981
0,5214	29,8726	0,9782		0,1493	22145,54727
0,3000	20,0000	1,0000		0,5250	22992,78129
0,3796	26,6500	0,8444		0,8799	23777,01477
0,4024	25,7500	0,9906		0,6376	24033,934
0,3000	20,0000	0,2500		0,5250	25632,3445
0,3000	20,0000	0,6250		0,1000	26566,54205
0,4154	26,5500	0,9494		0,2551	27832,03405
0,3991	25,5500	0,6944		0,3656	28003,71714
0,3114	21,1500	0,3531		0,3571	29019,29845
0,3095	21,8323	0,9768		0,1571	29526,80605
0,3095	21,8323	0,9768		0,1571	29526,80605
0,3764	24,3500	0,4994		0,2041	29963,99698
0,3146	23,1500	0,4244		0,6759	30531,44437
0,4414	29,9500	0,6156		0,5569	30980,49416
0,4186	27,0500	0,3044		0,2254	32213,85855
0,3276	23,2500	0,7581		0,1744	32401,65526
0,3569	28,3500	0,4844		0,8416	33583,1836
0,3081	23,4500	0,8519		0,4591	33630,22397
0,3926	27,5500	0,2931		0,5866	33774,84866
0,3309	25,8500	0,6869		0,6589	35187,51172
0,3959	29,1500	0,6194		0,1871	40488,82652
0,3168	28,9441	0,2563		0,8978	41043,73198
0,3439	27,7500	0,4544		0,4039	45880,20544
0,3406	28,9500	0,8256		0,4719	46857,31946
0,3070	29,8837	0,9871		0,7508	49472,58038
0,3328	29,7226	0,8243		0,1068	56202,30159
0,3000	30,0000	0,6250		0,5250	63519,11542

9.2 Ansys output data for study without eccentricity

P2 - P3@DS_Beta	P3 - P3@DS_Gamma	P4 - P3@DS_Tau	P15 - Fopb
0,89475	11,5	0,66625	500,3559587
0,88825	11,7	0,36625	550,8939044
0,87525	12,3	0,91375	642,5732001
0,94675	15,5	0,80125	665,7965114
0,76475	10,1	0,79375	729,1072357
0,94025	16,3	0,38125	799,7694077
0,71925	10,3	0,50125	967,0144476
0,86225	14,7	0,54625	1045,387684
0,84925	14,5	0,28375	1121,435261
0,90775	17,7	0,98875	1124,081145
0,82975	14,3	0,74125	1155,714359
0,79075	13,5	0,41875	1289,308535
0,93375	21,9	0,58375	1454,924027
0,72575	12,7	0,60625	1501,123027
0,92725	22,5	0,83875	1570,876463
0,71275	12,9	0,83125	1602,09474
0,68025	11,9	0,31375	1636,493074
0,80375	16,1	0,89125	1671,125413
0,56975	10,7	0,92125	1879,069887
0,85575	19,5	0,70375	1897,874346
0,57625	10,9	0,69625	1965,475234
0,88175	21,7	0,26875	2104,364209
0,91425	25,3	0,39625	2218,342183
0,83625	19,7	0,42625	2229,125284
0,75825	16,9	0,56875	2403,206034
0,92075	27,9	0,59875	2467,496314
0,90125	26,9	0,93625	2571,906542
0,63475	14,1	0,98125	2688,836404
0,59575	13,3	0,48625	2973,394758
0,49175	11,3	0,32125	3148,025329
0,81675	22,9	0,89875	3148,980659
0,67375	15,9	0,41125	3193,721392
0,84275	24,7	0,71125	3209,661646
0,69975	17,9	0,74875	3478,805637
0,40725	10,5	0,76375	3480,48275

0,61525	15,1	0,68125	3535,748674
0,73225	19,1	0,32875	3616,937855
0,43325	11,1	0,53125	3710,127202
0,77775	22,1	0,57625	3745,742928
0,86875	29,5	0,82375	3766,351227
0,81025	26,1	0,53875	4363,574057
0,70625	20,7	0,99625	4423,971183
0,74525	22,7	0,72625	4557,0655
0,82325	27,7	0,29875	4666,027882
0,77125	24,1	0,38875	4700,827133
0,47875	13,7	0,86875	4854,302885
0,60875	17,5	0,85375	4892,483448
0,54375	15,3	0,25375	5228,216822
0,78425	27,5	0,97375	5270,002499
0,69325	21,5	0,47875	5447,587101
0,60225	18,1	0,62125	5612,69526
0,45925	13,9	0,65125	5618,751807
0,66725	20,9	0,64375	5660,07427
0,79725	29,7	0,45625	6047,819187
0,62825	19,9	0,52375	6223,889276
0,73875	26,5	0,80875	6314,097362
0,53075	16,7	0,49375	6536,606217
0,36825	13,1	0,94375	6819,48547
0,32925	12,1	0,61375	6917,14357
0,75175	28,7	0,67375	7026,712065
0,45275	14,9	0,40375	7073,249459
0,68675	23,9	0,26125	7165,030255
0,65425	23,7	0,88375	7520,034697
0,33575	12,5	0,34375	7555,546959

0,49825	17,3	0,75625	7761,747473
0,58275	20,5	0,77125	7796,446962
0,64775	24,9	0,63625	8898,578137
0,53725	19,3	0,35125	8967,128172
0,62175	23,3	0,37375	9136,131245
0,43975	17,1	0,55375	10048,08217
0,38125	15,7	0,78625	10153,48275
0,66075	27,1	0,44875	10241,33684
0,51125	20,1	0,62875	10489,20174
0,51775	21,1	0,92875	10805,69447
0,64125	29,3	0,81625	12470,32405
0,56325	24,5	0,73375	12533,06042
0,40075	18,5	0,95875	13369,25941
0,52425	23,1	0,50875	13736,16243
0,55025	26,7	0,96625	15464,69363
0,42675	20,3	0,43375	16137,0933
0,58925	28,5	0,30625	16400,67236
0,55675	27,3	0,59125	16692,83964
0,30325	16,5	0,46375	16978,21995
0,41375	21,3	0,84625	17726,19232
0,35525	18,9	0,68875	17937,56977
0,36175	18,7	0,29125	18116,29015
0,46575	23,5	0,27625	19317,49409
0,30975	18,3	0,87625	19849,54739
0,47225	25,9	0,86125	21044,53747
0,48525	26,3	0,44125	22133,42557
0,50475	29,9	0,47125	26612,25062
0,42025	25,7	0,65875	27294,3866
0,37475	24,3	0,95125	28296,5749
0,44625	29,1	0,71875	31599,94758
0,32275	22,3	0,56125	31615,49854
0,34225	25,1	0,35875	39583,89199
0,38775	28,9	0,90625	39925,83014
0,39425	28,3	0,33625	40963,569
0,31625	25,5	0,77875	43139,0796
0,34875	28,1	0,51625	48656,01958

9.3 Ansys output data for study of ultimate capacity with eccentricity

P1ECC	P2Beta	P3Gamma	P8Moment
0,525	0,3	30	5000000
0,1	0,3	30	7400000
0,95	0,3	30	7500000
0,1	0,3	20	10000000
0,525	0,65	30	15000000
0,95	0,3	20	16500000
0,525	0,3	20	18900000
0,1	0,65	30	20000000
0,1	0,95	30	24000000
0,95	0,65	30	27000000
0,94575	0,56975	23,2725	31500000
0,525	0,3	10	38000000
0,1	0,3	10	40000000
0,95	0,3	10	40000000
0,525	0,65	20	43200000
0,1	0,65	20	45000000
0,95	0,65	20	53200000
0,525	0,95	20	60000000
0,525	0,95	30	62500000
0,95	0,95	30	63000000
0,1	0,95	20	113000000
0,95	0,95	20	120000000
0,1	0,65	10	143000000
0,525	0,65	10	150000000
0,95	0,65	10	180000000
0,1	0,95	10	340000000
0,525	0,95	10	345000000
0,95	0,95	10	362000000